ATMÓSFERA
https://www.revistascca.unam.mx/atm/

INSTITUTO DE CIENCIAS DE LA ATMÓSFERA Y CAMBIO CLIMÁTICO

EARLY ONLINE RELEASE

The following is a manuscript that has been peer-reviewed and accepted for publication in Atmósfera.

The text will be formatted and copy-edited, and the final published version may be different from this early online release.

It may be cited using the following DOI:

https://doi.org/10.20937/ATM.53322
Submission date: 01 August 2023
Acceptance date: 28 January 2024

The published manuscript will replace this preliminary version at the above DOI.

Atmósfera is a quarterly journal published by the Universidad Nacional Autónoma de México (UNAM) through its Instituto de Ciencias de la Atmósfera y Cambio Climático in Mexico City, Mexico. ISSN 2395-8812. https://www.revistascca.unam.mx/atm

The assessment of organic contaminants at a paint manufacturing site: implications for health risks and source identification

Sidali Khedidji,[1,2*] Catia Balducci,[3] Lyes Rabhi,[2,4,5] Angelo Cecinato,[3] Riad Ladji,[4,5] and Noureddine Yassaa,[2,6].

[1] *Faculté des Sciences et des Sciences Appliquée (FSSA), Université de Bouira, 10000, Bouira, Algérie,* https://orcid.org/0000-0001-5221-8851

[2] *Laboratoire d'Analyse Organique Fonctionnelle, Université des Sciences et de la Technologie Houari Boumediene (USTHB), BP 32, El-Alia, Bab Ezzouar, 16111 Alger, Algérie.*

[3] *Institute of Atmospheric Pollution Research (CNR-IIA), National Research Council of Italy, Via Salaria, km 29.3, P.O. Box 10, 00015, Monterotondo, RM, Italy.*

[4] *Centre de Recherche Scientifique et Technique en Analyses Physico-chimiques (CRAPC). Zone Industrielle, BP 384 Bou-Ismail, Tipaza, Algeria*

[5] *Unité de Recherche en Analyses Physico-Chimiques des Milieux Fluides et Sols –(URAPC-MFS/ CRAPC), 11, Chemin Doudou Mokhtar, Ben Aknoun – Alger, Algeria.*

[6] *Commissariat aux Energies Renouvelables et à l'Efficacité Energétique, CEREFE, 12 Rue Docteur Slimane Asselah, Telemly, Algiers, Algeria.*

**Corresponding author: E-mail address: skhedidji@gmail.com*

Received: yyyy mmm dd Accepted: yyyy mmm dd

SHORT TITLE

Assessment of PBF and GBF

HIGHLIGHTS

- The 5- and 6-ring PAHs were predominant in airborne particles, while the 2- and 3-ring PAHs were much higher in the gaseous phase.
- Correlations between individual PAHs have been affected by changes in emission sources.
- ILRC exceeded the USEPA levels established for health preservation.

GRAPHICAL ABSTRACT

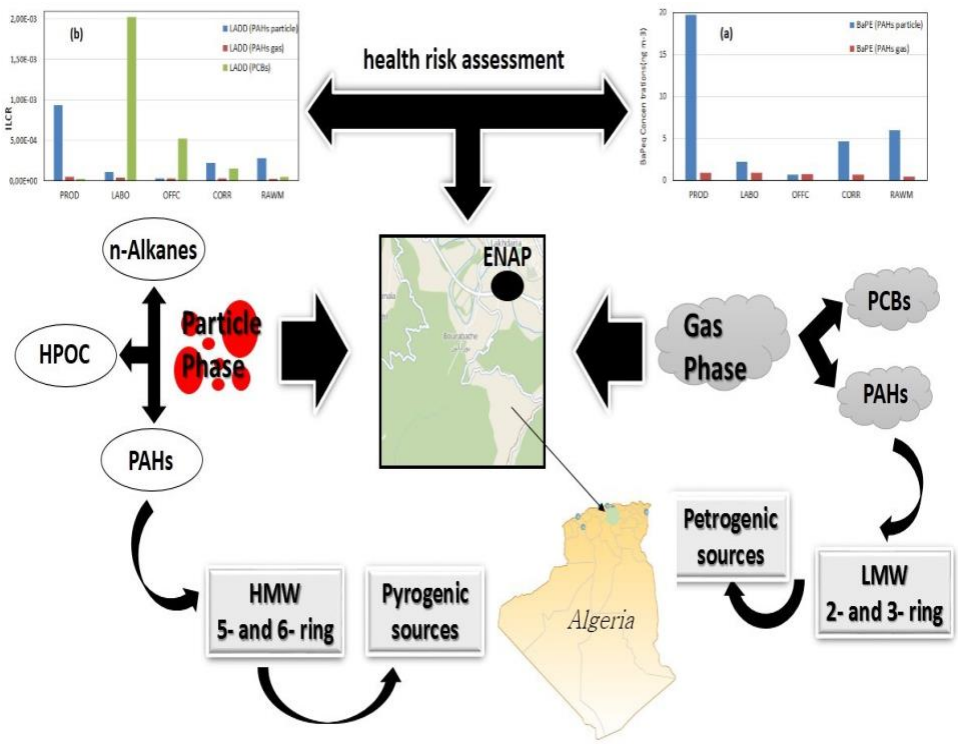

ABSTRACT

The daily variation of organic contaminants, both gaseous and associated with suspended particulate matter, was investigated within the National Company of Paintings estate in Lakhdaria, Algeria, spanning the period 2014-2015. The research emphasizes the chemical characterization of suspended particulate matter, analyzing a range of organic compounds, including n-alkanes, polycyclic aromatic hydrocarbons (PAHs), and highly polar organics (HPOC), such as phthalate esters and heterocyclic compounds. Vapours of PAHs and polychlorobiphenyls (PCBs) were also analyzed. Low molecular weight compounds were primarily associated with the gas phase (2-ring PAHs, approximately 95%; 3-ring PAHs, around 70%), while high molecular weight congeners were mainly associated with the particle phase (6-ring PAHs, 55%). The concentrations of PCBs (ranging from 0.6 to 42 ng m^{-3}) were higher than those reported in other cities in Algeria and Europe.

The source reconciliation of organic contaminants through principal component analysis (PCA) demonstrated that the primary sources were petroleum combustion, industrial manufacturing, tobacco smoking, and vehicular traffic. The significance of tobacco smoke was further confirmed by the analysis of PAHs diagnostic ratios. The variations in diagnostic ratio rates between gaseous and particulate PAHs were attributed to distinct contributions from sources such as industrial processes. Health risks for workers exposed to PAHs and PCBs in PM_{10} were quantitatively assessed in terms of Benzo[a]pyrene equivalent concentration (BaPeq) and incremental lifetime cancer risk (ILCR). ILCR presents novel findings, showcasing heightened risks among workers exposed to specific PAHs within production areas, whereas that related to PCBs suggested a high potential health risk for laboratory workers.

Keywords: Organic compounds, PAHs, paint manufacturing, Source apportionment, ILCR

RESUMEN

La variación diaria de contaminantes orgánicos, tanto gaseosos como asociados a material particulado suspendido, fue investigada dentro del patrimonio de la Compañía Nacional de Pinturas en Lakhdaria, Argelia, durante el periodo 2014-2015. La investigación enfatiza la caracterización química del material particulado suspendido, analizando una gama de compuestos orgánicos, incluyendo n-alcanos, hidrocarburos aromáticos policíclicos (HAP), y compuestos orgánicos

altamente polares (COAP), como ésteres de ftalato y compuestos heterocíclicos. También se analizaron vapores de HAP y bifenilos policlorados (PCB). Los compuestos de bajo peso molecular estaban principalmente asociados con la fase gaseosa (HAP de 2 anillos, aproximadamente el 95%; HAP de 3 anillos, alrededor del 70%), mientras que los congéneres de alto peso molecular estaban principalmente asociados con la fase de partículas (HAP de 6 anillos, 55%). Las concentraciones de PCB (que oscilaban entre 0.6 y 42 ng m-3) fueron más altas que las reportadas en otras ciudades de Argelia y Europa.

La reconciliación de fuentes de contaminantes orgánicos a través del análisis de componentes principales (ACP) demostró que las fuentes primarias eran la combustión de petróleo, la fabricación industrial, el tabaquismo y el tráfico vehicular. La importancia del humo de tabaco fue confirmada además por el análisis de las relaciones diagnósticas de los HAP. Las variaciones en las tasas de relaciones diagnósticas entre los HAP gaseosos y particulados se atribuyeron a contribuciones distintas de fuentes como procesos industriales. Los riesgos para la salud de los trabajadores expuestos a HAP y PCB en PM_{10} fueron evaluados cuantitativamente en términos de concentración equivalente de Benzo[a]pireno (BaPeq) y riesgo incremental de cáncer a lo largo de la vida (ILCR). El ILCR presenta hallazgos novedosos, mostrando riesgos elevados entre los trabajadores expuestos a HAP específicos dentro de áreas de producción, mientras que el relacionado con los PCB sugirió un alto riesgo potencial para los trabajadores de laboratorio.

Compound symbols: PAHs, polycyclic aromatic hydrocarbons; HPOCs, highly-polar organic compounds; PAEs, phthalate esters; PCBs, Polychlorobiphenyls; Nap, Naphthalene; 1-Me-Nap, 1methyl-naphthalene; 2-Me-Nap, 2 methyl-naphthalene; Me-2-Nap, methyl-2-naphthalene; Acy, acenaphthylene; Ace, acenaphthene; FA, Fluorene; Phe, phenanthrene; Ant, anthracene; Me-Phe, methyl-phenanthrene; Flu, fluoranthene; Pyr, pyrene; Me-Flu/Pyr, methyl-fluoranthene/pyrene; BcPhe, benzo(c) phenanthrene; BaA, Benzo(a)anthracene; Chr, Chrysene; Me-Chr, methyl-chrysene; BghiF, Benzo(ghi)Fluoranthene; CPPyr, cyclopent(cd)pyrene; BbF, benzo(b)fluoranthene; BjF, benzo(j)fluoranthene; BkF, benzo(k)fluoranthene; BaF, benzo(a)fluoranthene; Pery, Perylene; BeP, Benzo(e)pyrene; BaP, Benzo(a)pyrene; DBahA, dibenzo(a,h)anthracene; IcdP, indeno(1,2,3-cd)pyrene; BghiP, benzo(ghi)pyrene; DBalP, dibenzo(a,l)pyrene; DBaeP, dibenzo(a,e)pyrene; DBaiP, dibenzo(a,i)pyrene; DBahP, dibenzo(a,h)pyrene; (LMW)-PAHs = low molecular weight PAHs; (HMW)-PAHs = high molecular weight PAHs; NIC, nicotine; COT, cotinine; CAF, caffeine; ACR, acridine; CAR, carbazole; ANTQ, anthraquinone; DEET, N,N-diethyl-meta-toluamide; NP, nonylphenol; DMP, dimethyl phthalate; DEP, Diethyl phthalate; DBP, dibutyl phthalate; DEHP, di-2-ethylhexyl phthalate; DOP, di(n-octyl) phthalate.

Abbreviation: PBF: Particulate bound fraction; GBF: Gas bound fraction; PCA: Principal compound analysis; ILCR: Incremental lifetime cancer risk; LADD: Lifetime average daily dose.

1. Introduction

In recent years, numerous investigations have been carried out over the world focusing on indoor air pollution, since the importance has raised of the lifetime (>80% of the total) spent by people at home and work places in modern urban areas (Baya et al. 2004; Ohura et al. 2009), especially during the Covid-19 pandemic period. Indeed, the poor air quality of interiors is a source of both acute and chronic health problems; hence, the determination of indoor air chemical composition is crucial to protect public health (Romagnoli et al. 2014). According to the last report of the World Health Statistics published in 2021, near 4.3 million deaths per year are caused by indoor pollution (WHO 2021).

The previous studies scrutinized VOC (Volatile Organic Compound) concentrations in a paint factory, gauging associated health risks. It established Hazard Quotients (HQ) to evaluate potential health impacts. Benzene, n-nonane, trichloroethylene, and tetrachloroethylene surpassed safe levels throughout the paint production. Additionally, Xylene, ethylbenzene, and toluene frequently surpassed permissible limits, except in specific areas such as the laboratory (Ghobakhloo et al. 2023). Furthermore, several studies emphasize the carcinogenic potential of substances such as benzene and ethylbenzene, notably prevalent in automobile manufacturing settings, including diverse workshops. This conclusion is based on the estimated Lifetime Cancer Risk (LCR) exceeding the set thresholds by the US EPA (Khoshakhlagh et al. 2023a). These findings underscore the need for stringent control measures and heightened safety protocols in the factory to mitigate health hazards.

The sensitivity analysis scrutinized essential variables affecting to the estimated risks associated with exposure to formaldehyde at work. The concentration of formaldehyde stood out as the primary factor influencing both cancer-related and non-cancer-related risks. Exposure duration and frequency also played significant roles in carcinogenic risk, while exposure time was pivotal for non-cancer-related risk. Body weight showed minimal influence on risk levels. This investigation emphasizes the crucial role of regulating formaldehyde concentrations to minimize health risks for employees who are exposed to it (Khoshakhlagh et al. 2023b).

Among the organic compound families, polycyclic aromatic hydrocarbons (PAHs) represent a significant concern due to their potential carcinogenic and mutagenic effects on human health. PAHs primarily result from incomplete combustion or pyrolysis of organic matter, including

petroleum, biomass, wood, coal, and tobacco (Yassaa and Cecinato 2005; Khedidji et al. 2013). Extensive research has focused on various aspects of PAHs, encompassing their partitioning between gas and particle phases, spatial and temporal patterns, size distribution, and associated health risks (Wei et al. 2015; Kim et al. 2013; Wu et al. 2014; Cecinato et al. 2014a). PAHs occur in the atmosphere as complex mixtures of congeners with different molecular weights; lighter PAHs (with 2-3 aromatic rings) predominantly exist in the vapor phase, while higher molecular weight PAHs (4-6 rings) tend to adsorb onto particulate matter (Sarti et al. 2017).

Another class of concern is polychlorobiphenyls (PCBs), which, being semi-volatile, primarily exist in the gas phase. Their toxicity, persistence, and potential carcinogenic/mutagenic effects have raised significant apprehension (Yenisoy-Karakaş et al. 2012). Despite substantial research into PAHs and PCBs in outdoor air, studies examining their presence in indoor environments are notably lacking when compared to the extensive literature. In Algeria, while there's been some exploration of PAHs presence in outdoor settled dust, considerable gaps remain, especially concerning suspended particulates (PM_{10}). Moreover, there's a lack of information regarding the indoor air quality within factories.

This paper presents the findings of an investigation conducted within an Algerian painting factory, where the materials used in manufacturing processes and their by-products were expected to potentially deteriorate air quality and endanger workers' health. The study focused on analyzing n-alkanes, PAHs, and highly-polar organic compounds (HPOC), including phthalate esters and heterocyclic compounds containing nitrogen and oxygen. The targeted substances were anticipated not only to assess the pollution levels within the factory premises and the corresponding exposure of workers to toxicants but also to elucidate the sources of pollution. Such insights are instrumental in endeavors to enhance air quality. Additionally, this study sheds light on the contributions of manufacturing processes in releasing and dispersing organic contaminants into the air.

2. Experimental

2.1. Sampling site and locations

The National Company of Paintings (thereafter named ENAP) is an Algerian Public Company. Its core activity is the production of organic coatings, including paints, varnishes, resins, adhesives, and emulsion driers. ENAP is comprised of six manufacturing plants deployed in Oued Smar and

Cheraga (Algiers), Lakhdaria, Oran, Sig (Mascara), and Souk-Ahras. The unit of Lakhdaria (the subject of this study) is considered as the biggest in the country, reaching the production capacity of 125,000 tons in paintings and 57,000 tons in semi-finished products (resins, emulsions, and drying agents). The estate is spread over an area of 8 hectares and employs around 340 workers. The ENAP estate is located at about 72 km south-east of Algiers, approximately 5 km outside the city of Lakhdaria (latitude 36°37’00’’ N, longitude 03°35’00’’ E) and 45 km west of the Bouira Province capital.

The sampling site was situated at an altitude of 203 m above sea level and at the distance of ~50 m from the National Algerian Highway. A view of the ENAP factory with the sampling points across the premises is provided in Figure 1.

Our study consisted in chemical characterization of gaseous and particulate organics affecting the atmosphere in the ENAP premise. As shown in Supplementary Information (Table SI), the five locations were premise interiors, namely: *i)* laboratory (LABO); *ii)* workshop of the paint production (PROD); *iii)* corridor of the production workshop (CORR); *iv)* workshop of stocked raw materials (RAWM); and *v)* offices (OFFC). Though close each one another, the locations were well physically separated, so that they were representative of distinct micro-environmental contours where workers used to operate.

2.2.Sample collection

Suspended particulate matter was collected every working day between April and May 2014, except for weekends during which the production process was stopped. Collection was operated at medium volume conditions (flow rate = 1.26 m^3 h^{-1}) and restricted to the PM_{10} fraction, i.e., particles with an aerodynamic diameter lesser than 10 μm, by using a particle size selective inlet. Samples were enriched onto pure quartz fibre filters; each collection started at 8:00 h and lasted 24 h.

Vapour compounds were enriched from air using *Analyst-2* type passive sampling cartridges (purchased from Marbaglass, Rome, Italy) that were positioned ca. 5 m above ground. This kind of diffusive sampler operates at a virtual flow rate of 18.5 mL min^{-1}, quite independently of the PAHs compound (Bertoni et al. 2001). The cartridge exposure lasted 5 months, starting in October 2014 and ending in February 2015.

After collection, both quartz filters and diffusive samplers were sealed in polyethylene boxes, wrapped with aluminum foils and stored in a freezer at a low temperature (-16°C) until chemical processing. Filter and cartridge blanks were co-located in the field with operating collection devices, in order to account for possible contamination occurring in sample handling, preparation and chemical analysis.

The PM_{10} concentration in the air was determined gravimetrically, through weighting filters with a microbalance (OHAUS EX125) with a precision of 10 µg, after 48 h conditioning at constant temperature (22 °C) and humidity (45 % RH). Finally, the filters were stored at −20 °C until chemical processing.

2.3. Analytical procedures

First, chemical characterization of particulate bound fraction (PBF) was performed using a protocol extensively described elsewhere (Gheriani et al. 2022; Khedidji et al. 2017a; Romagnoli et al. 2019). Briefly, prior to the solvent extraction the filters were fortified with a mixture of internal standards; they were: for n-alkanes, perdeuterated tetradecane ($C_{14}D_{30}$), hexadecane ($C_{16}D_{34}$), eicosane ($C_{20}D_{42}$), tetracosane ($C_{24}D_{50}$), triacontane ($C_{30}D_{62}$); for PAHs, acenaphthene-D_{10}, phenanthrene-D_{10}, fluoranthene-D_{10}, benz[a]anthracene-D_{12}, benzo[a]pyrene-D_{12}, dibenz[a,h]anthracene-D_{14} and dibenzo[a,i]pyrene-D_{14}; for HPOCs, nicotine-D_4, cocaine-D_3, and caffeine-$^{13}C_3$, di-n-propylphthalate DPrPE and dicyclohexylphthalate DcHxPr. These compounds were added at known concentrations to samples before extraction and analysis, help assess the efficiency of the extraction and analysis processes. By comparing the amount of added standard to the amount recovered, analysts can determine the analytical recovery efficiency. They're added at a constant concentration to both calibration standards and samples. The ratio of the analyte's signal to the internal standard's signal is used to calculate the concentration of the analyte in the sample.

As for the sample treatment, the organic fraction was recovered by means of an accelerated solvent extractor (ASE-150, Dionex, purchased from Thermo Scientific, Rodano MI, Italy) using a mixture of acetone, *n*-hexane and toluene (60:30:10 in volume; 10 mL, 4 times, 18 min each) as solvent. Neutral alumina (for column chromatography, 3.0 g, partly deactivated with 2.5% of water, provided by Carlo Erba Reagenti, Rodano MI, Italy) was employed to clean-up and fractionate the sample extracts. For this purpose, the extracts were reduced close to dryness at room temperature

under a gentle flow of nitrogen, transferred to the top of the alumina column and eluted by means of trimethylpentane (TMP, 10 mL), TMP/dichloromethane (20:80, 10 mL) and dichloromethane/acetone (50:50, 12 mL), in sequence. Three fractions of raising polarity were collected, the first one containing *n*-alkanes and non-polar aliphatic hydrocarbons, the second including PAHs, and the third one HPOCs. The three eluates were reduced to dryness and back dissolved with toluene (the 2nd fraction) or chloroform.

The procedure adopted for gaseous bound fraction (GBF) followed the protocol established by Bertoni et al. (2001). Indeed, each sample (i.e., the adsorbing graphitized carbon lodged in the diffusive cartridge) was transferred into a borosilicate vessel, fortified with a mixture of internal standards containing naphthalene-D_8, 2-methylnaphthalene-D_8, fluorene-D_{10}, phenanthrene-D_{10}, anthracene-D_{10}, pyrene-D_{10} and chrysene-D_{12}, and finally extracted with toluene (2 mL).

Instrumental analyses were carried out by means of a *Trace GC Ultra* gas chromatograph equipped with an *AS-2000* auto-sampler and coupled with a *Trace DSQ* quadrupole mass spectrometer (all purchased from Thermo, Rodano MI, Italy). Chemical determinations were performed by using a DB5-MS type column (L = 30 m, i.d. = 250 µm, film thickness = 0.25 µm; purchased from CPS Analytica, Milan, Italy).

Distinct oven temperature programs were applied for GC analyses. In particular,

a) for PAHs, *n*-alkanes and PCBs fractions: starting temperature =70 °C (1.25 min), +20 °C/min to 200 °C (2 min), +10 °C/min up to 280 °C (10 min), +5 °C/min to 290 °C (15 min);
b) for HPOCs: starting temperature = 70 °C (1.25 min); +15 °C min^{-1} to 175 °C (2 min), +5 °C min^{-1} to 280 °C (10 min); +5 °C min^{-1} up to 285 °C (18 min).

In both cases, helium (0.8 mL min^{-1}) was adopted as carrier gas, and injection was operated in split-less mode (1.2 min).

The mass spectrometer system was run in electron impact, selected ion monitoring mode (ion source energy=70 eV; three or four diagnostic ion traces per analyte), and the GC/MS data were acquired by means of dedicated software (*Excalibur*) purchased from Thermo.

2.4. Quality assurance of the analytical method

Before sample collection, quartz filters were backed in a furnace (450°C, 4h) to remove organic impurities and were stored at 40–50% relative humidity over 48 h, weighted and sealed individually in polyethylene holders until use. The instrument underwent calibration, and blanks were analyzed prior to each sample series to ensure accuracy. Field blanks were treated using the same conditions and procedures as the samples to act as a control against potential contamination. Samples were analyzed in triplicate, and peak areas were normalized to corresponding reference compounds—perdeuterated congeners spiked into samples just before solvent extraction served as these references. Calibration curves for the targeted compounds were established using eight standard mixture solutions. Each mixture, injected three times for various polarity fractions, covered concentrations ranging from 25 to 0.1 ng μL^{-1} for each target compound, with a constant internal standard content of 1.0 ng μL^{-1}. The replicates showed relative standard deviations ranging from 4% to 10% for all analytes, meeting set quality criteria. Calibration curves, covering a concentration range of 0.005 to 4.0 mg ML^{-1}, exhibited strong linearity with coefficients of determination (R^2) exceeding 0.978, indicating a robust linear relationship between concentration and response. Method sensitivity, expressed as the limit of quantification (LOQ), was determined to be superior to 0.060 ng/sample for BaA and 0.427 ng/sample for IcdP. These values denote the lowest reliable quantifiable concentrations for these compounds using this analytical method. Overall, this methodology employed stringent calibration, quality control measures, and sensitivity assessments, ensuring precise and reliable quantification of target compounds in the samples.

3. Results and discussion

3.1. PM_{10} mass concentrations

Table I shows the mean atmospheric concentrations of PM_{10} as a whole and those of particulate compounds, namely *n*-alkanes, PAHs and polar substances, as well as those of gaseous PCBs and PAHs, observed at the five locations inside the factory. Figure 2 shows the PM_{10} mass concentration patterns.

According to Table I, the mean PM_{10} concentration reached 46.7 µg m^{-3} in PROD, 56 µg m^{-3} in LABO, 42 µg m^{-3} in OFFC, 59 µg m^{-3} in CORR, and 95 µg m^{-3} in RAWM. In RAWM, the PM_{10} rates ranged 73÷144 µg m^{-3}, exceeding 2-5 times those recorded elsewhere. The maximum observed at RAWM probably depended on limited air ventilation and on primary materials

accumulated there, i.e., fillers, pigments, binders and solvents used in the manufacture of paints, and used as fine particles insoluble in the suspension medium (Can et al. 2015). Throughout the PM_{10} concentration rates, only 10 exceedances occurred of the limit value of 50 µg m^{-3} set by Algerian legislation (PDRA-ED, 2006) and European normative (Directive 2008/50/EC).

3.2. Occurrence and composition of particle bound fraction (PBF)

3.2.1. n-Alkanes

Total *n*-alkanes (comprised of 21 homologues from tetradecane [C_{14}] to tetratriacontane [C_{34}]) associated with PM_{10} fraction ranged between 114 ng m^{-3} (in the raw materials room) and 484 m^{-3} (production area). Similar trends were observed at all sampling sites; C_{21} and C_{22} were the most abundant homologues during the whole period of investigation, while C_{14}, C_{15} and C_{30}-C_{34} were the poorest ones (Fig. 3).

This pattern was indicative of anthropogenic emissions prevailing vs. natural sources, as confirmed by the values (~1.2) of the n-alkane Carbon Preference Index (CPI), calculated as the sum of the concentrations of odd carbon number alkanes divided by the sum of the even carbon number alkanes concentrations (Alves et al. 2014; Gheriani et al. 2022). The formulas we applied are:

$$CPI = \sum(C_{20}\text{-}C_{32})/\sum(C_{21}\text{-}C_{33}) \quad (1)$$

3.2.2. Polycyclic Aromatic Hydrocarbons (PAHs)

The concentrations of twenty-six Polycyclic Aromatic Hydrocarbons (i.e., parent compounds and methyl-derivatives from phenanthrene to dibenzopyrenes) in the paint manufacturing plant are reported in Figure 4.

Total PAHs associated with the PM_{10} ranged from ~7.0 ng m^{-3} to ~35 ng m^{-3}. An important spatial gradient was observed, with high concentrations in the production room and low concentrations in the office, which was situated in a relatively clean atmosphere. Besides, total

PAHs reached 15.4 ng m^{-3}, 12.8 ng m^{-3} and 16.3 ng m^{-3}, respectively, in the corridor, raw materials and laboratory rooms. While the raw material and corridor rooms were close to the production area, the PAHs exposure inside the laboratory was low; on the other hand, the special profile of PAHs seemed to indicate that this location was affected by peculiar pollution sources; in particular, dibenzopyrenes (DBPs) touched their maximum in the laboratory, while they were almost absent in the office. Indeed, the whole of the paintings, methods and operations were tested there, which could characterize this microenvironment within the factory.

To enhance the significance of our findings, we compared the concentrations of PAHs within our paint manufacturing plant with those observed elsewhere in Algeria and all over the world. The levels of PAHs (07-35 ng m^{-3}) in this study were clearly higher than those reported in several Algerian locales, such as the industrial zone of Rouiba–Réghaia (Ladji et al. 2009), industrial sites in Bouira province (Khedidji et al. 2017a), Bourouba city (Rabhi et al. 2018), and the coastal area in Bou Ismaïl (Khedidji et al. 2020) and in other locations of the world at Hamadan city in western Iran (A. Nadali et al. 2021) and German states (H. Fromme et al.2023). They are of the same order of magnitude as those recorded in Ketu- Nigeria and Shahryar City in Iran (R. Alani et al. 2021; M. Kermani et al 2023). However, they were lower than concentrations documented in the industrial center of Hassi-Messaoud and the urban area of Touggourt (Yassaa and Cecinato 2005; Gheriani et al. 2022), Santiago Coachochitlán town in the State of Mexico and Ardabil city in northwestern Iran (B. L. Valle-Hernández et al. 2021; R. Rostami, et al. 2019).

Benzo(a)pyrene is often selected as the primary indicator for the entire PAHs group and serves as a marker for overall exposure to suspended particulate carcinogens, consequently reflecting associated health risks. In our study, the average concentration of BaP was ranged from 0.26 to 0.83 ng m^{-3}. The BaP average at the indoor site exceeded those previously reported elsewhere in Algeria such as industrial sites in Bouira (0.03-0.27 ng m^{-3}) (Khedidji et al. 2017a), Bourouba city (0.12-0.42 ng m^{-3}) (Rabhi et al. 2018) and industrial zones Rouiba–Réghaia (0.04-0.29 ng m^{-3}) (Ladji et al. 2009), and was clearly higher compared to those reported at Hamadan city in western Iran (0.001- 0.007 ng m^{-3}), German states (0.052-0.065 ng m^{-3}) and Ketu in Nigeria (0.06–0.08 ng m^{-3}) (A. Nadali et al. 2021; H. Fromme et al.2023; R. Alani et al. 2021). Moreover, levels of BaP in ENAP was lower than those recorded at the urban area of Touggourt (0.83-2.24 ng m^{-3}) and Santiago Coachochitlán town in the State of Mexico (6.5-15.9 ng m^{-3}) (Gheriani et al. 2022; B. L. Valle-Hernández et al. 2021).

3.2.3. Highly-polar organic compounds (HPOCs)

Total contents of polar contaminants (comprising five heterocyclic compounds, six phthalate esters and three nitrogen- and oxygen-containing compounds) ranged from 147 ng m^{-3} in the office room up to 424 ng m^{-3} inside the paint production zone, following a trend similar to *n*-alkanes. Among highly polar compounds, nicotine was predominant in all interiors, particularly in the production room and corridor; there, it accounted for 98% and 96%, respectively, of the total of polar substances (Fig. 5). This behavior was influenced by the huge tobacco smoking during work time (more in the production zone and in corridors than elsewhere), and also by the higher temperature indoors compared to outdoors; that occurred despite the concentrations determined in air which could be somehow underestimated due to nicotine volatility (Eatough et al. 1989; Morawska and Zhang 2002).

Levels of nicotine in the production area (141- 414 ng m^{-3}) were clearly higher than previously reported in some industrial sites at the bouira province 9.5-137 ng m^{-3}), the industrial zone Rouiba–Réghaia (9.4-16.8 ng m^{-3}), San Francisco-USA (0.412 -7.628 ng m^{-3}), Birmingham-UK (0.541-5.489 ng m^{-3}), Msida- Malta (6.761-81.537 ng m^{-3}) (Khedidji et al. 2013; Ladji et al. 2014; Aquilina et al. 2021), and exhibited the same magnitude and variability that was observed in European countries such as Germany (0.03-0.97 μg m^{-3}) and Portugal (0.04-0.56 μg m^{-3}) (Henderson et al. 2023). However, they were lower to those recorded in Barcelona (1.15 μg m^{-3}), Baltimore (1.42 μg m^{-3}), Toronto (2.74 μg m^{-3}), and Romania (11.1 μg m^{-3}) (Feliu, et al. 2020; Torrey et al. 2015; Zhang et al. 2015; Henderson et al. 2023).

The paint production zone was characterized also by high concentrations of phthalate esters PAEs, i.e., 10 ng m^{-3} vs. ~1.0 ng m^{-3} reached in the office. Among the six phthalates investigated, diethyl homologue (DEP) was all the-time the most important, though it is more volatile than dibutyl and diethylhexyl congeners. PAEs concentrations could be influenced, especially in the corridor, by additional emission sources like plastics, detergent bases and aerosol sprays used for cleaning (Tran and Kannan 2015). It is worth mentioning that PAEs are gaining concern as endocrine disruptors and toxic; besides, their combustion by-products display toxic properties (Gao and Wen 2016).

3.2.4. Polychlorobiphenyls (PCBs)

PCBs co-exist in the atmosphere as vapors and are adsorbed on atmospheric particles (Gregoris et al. 2014). In this study, PCBs could be investigated only in the vapor phase, due to the minimum concentrations (<<0.1 ng m^{-3}) reached by these compounds in airborne particulates. Indeed, in ambient air PCBs exhibit a marked preference of the gaseous phase except for the most chlorinated homologues (>Cl_8), and only congeners from Cl_3- to Cl_6-CBs were detected in this study. Despite the method applied to collect and measure PCBs allowed drawing only semi-quantitative information, large differences among the five locations were put in the evidence.

The average concentration of gaseous PCBs was ca. 0.6 ng m^{-3} in PROD, 42 ng m^{-3} in LABO, 11 ng m^{-3} in OFFC, 3.2 ng m^{-3} in CORR and 11 ng m^{-3} in RAWM. The maximum concentrations were observed in the laboratory, which was roughly 13 and 4 times more polluted than corridors and offices, respectively.

The results found in this study exceeded those reported in other Algerian cities such as in the suburban coastal zone of Bou Ismail (~0.03÷0.07 ng m^{-3}), Baraki (0.10÷0.15 ng m^{-3}, Moussaoui et al. 2012) and at the industrial cement plant in Sour el Ghozlane (~0.02 ng m^{-3}, Khedidji et al. 2017b). There were also much higher than in the European cities of Brescia (Colombo et al. 2013) and Madrid (Barbas et al. 2018), but they were of the same order of magnitude of the heavily industrialized region of Kocaeli city in Turkey (4.2÷6.1 ng m^{-3}, Cetin et al. 2018).

3.2.5. Gaseous PAHs

Mean indoor concentrations of individual gaseous PAHs (GBF, expressed in ng m^{-3} units) in the five interiors investigated are provided in Figure 6.

The sum of non-alkylated and methyl substitute gaseous PAHs reached ca. 2,329 ng m^{-3} in PROD, 1,946 ng m^{-3} in LABO, 1,797 ng m^{-3} in OFFC, 1507 ng m^{-3} in CORR and 834 ng m^{-3} in RAWM. Hence, gaseous PAHs were much more abundant than the particulate ones at all the locations of the factory premises.

Total PAHs at the PROD were significantly higher compared to the other sites, hence the paint manufacturing was suspected to be an important source of gaseous PAHs, because of the use of several solvents, thinners, varnishes and adhesives in this workshop. Low PAHs concentrations

were measured in the raw materials workshop, presumably due to the contents of materials used there, which were characterized by particulate rather than by vapours (see the section 3.1.). Another interesting finding was that PAHs concentrations measured in the office were higher than in the corridor, in accordance with odors perceived during the delivery of the samples, because the small office room suffered from insufficient ventilation, unlike LABO and COR.

Nap, 1-Me Nap, 2-Me Nap and Me-2-Nap were the principal PAHs occurring among the 13 ones measured in the gas phase, and accounted for 42%, 15%, 8%, and 29% of the total, respectively. Naphthalene and their methylated derivatives are released by primary sources and react with OH radicals and NO_x to produce secondary organic aerosols (SOA) (Chen et al. 2016). Further, several studies have simulated the gas-phase chemistry and particle-phase organic aerosol formation starting from naphthalene and alkyl naphthalene emission (Nishino et al. 2012; Lu et al. 2005 ; Kautzman et al. 2010).

In our study, the volatile Nap was found with mean concentrations of 691 ng m^{-3}, and a range of 404- 900 ng m^{-3}. Similar results were reported in a comprehensive compilation of measurement results performed by German states and Ardabil city in northwestern Iran (H. Fromme et al.2023; R. Rostami, et al. 2019). However, they were clearly higher than previously reported at the residence area in Algiers (173-265 ng m^{-3}) and Hamadan city in western Iran (1.852- 40.025 ng m^{-3}) (Khedidji et al. 2013; A. Nadali et al. 2021).

3.3. PAHs distribution according to aromatic rings

Figure 7 shows the PAHs percentage distribution according to aromatic ring number both in the gaseous and particulate phases. The 6-ring congeners accounted for 65% of total PAHs in PROD, 61% in RAWM and 49% in COR and were the most abundant species of particulate phase, followed by 4-ring compounds, which accounted for 51% of the total in LABO and 48% in OFFC; on the other hand, the gaseous phase was dominated by the 2-ring PAHs, ranging from 93% in OFFC to 97% in LABO. Besides, in the gas phase 2-ring PAHs exceeded the 3-ring and 4-ring homologues by factors up to up to 31 and 44, respectively. Instead, when particulate PAH percentage profiles were compared, the 6-ring group was, on average, 6, 5 and 4 times more, respectively than the 3-ring group in PROD, RAWM and CORR; besides, the 4-rings PAHs were twice 3-rings PAHs.

In conclusion, high molecular weight (HMW) PAHs (i.e., the 5- and 6-rings ones) were relatively rich in the particulate phase, whereas low molecular weight (LMW) PAHs (2-rings) were predominant in the gas phase, similarly to the behavior of organic fuel burning (Tobiszewski and Namieśnik 2012). In particular, 4-rings PAHs have been related to coal combustion (Hu et al. 2019; Li et al. 2016). The important concentrations of 2-rings PAHs in the gas phase could depend on high temperature inside the premise, which promoted volatilization vs. adsorption on soot. In addition, the important occurrence of semi-volatile PAHs (4 rings PAHs) as particulate could depend on the total relative abundance in the air and phase partition (Pandey et al. 2011).

3.4. Diagnostic ratios (DRs) of gaseous and particulate PAHs

The emission percentage profile associated with PAHs sources such as industrial processes, petrol and diesel oil combustion, coal and wood burning (Mostert et al. 2010) depends on the mechanisms leading to PAHs release/formation. For instance, the low molecular weight PAHs are usually produced during low temperature processes; these PAHs are multi-alkylated and molecules contain fewer aromatic rings than pyrogenic PAHs (Zhang et al. 2008); besides, they can already occur in the fuels. On the other hand, high molecular weight PAHs are released by high temperature processes, such as fueled engine combustion. In order to determine the major sources of gaseous and particulate PAHs in five locations, we proceeded to calculate the concentration ratios of PAHs pairs (Khedidji et al. 2013, 2020; Balducci et al. 2014; Cecinato et al. 2014b).

Among the diagnostic ratios (DRs) commonly examined for source identification, our concern was focused on the following ones: Phe/(Phe+Ant); Flu/(Flu+Pyr); BaA/(BaA+Chr) BeP/(BeP+BaP); IcdP/(IcdP+BghiP); and (alkylate PAHs/parent PAHs) (Table II).

According to DRs rates, no significant differences were found between the five environments investigated inside the premise. The Ant/(Phe+Ant) ratio ranged from 0.05 to 0.08 for gas phase and from 0.37 to 0.53 for the particulate phase. Distinct values have been documented (rates <0.1 or >0.1, respectively) to distinguish petrochemical emissions (e.g. lubricant oils and petrol-derived fuels) from solid fuel exhausts (coal) (Tobiszewski and Namieśnik 2012).

Furthermore, the parent/alkylated PAHs ratio is considered as an index of petrogenic source contribution, because alkylated PAHs in petroleum products are more abundant than parent PAHs (Dobbins et al. 2006 ; Zakaria et al. 2002). The Nap/Me-Nap ratio was calculated for the gas phase, and Chr/Me-Chr ratio for particulate phase. Values of Nap/Me-Nap calculated at PROD, OFFC and CORR (0.5-0.9) and to a lesser extent those at the laboratory (1.1) and raw material workshop (1.0) put into evidence the contribution of petrogenic sources for gaseous PAHs, while Chr/Me-Chr ratio rates (1.0 to 1.6) confirmed that particulate PAHs originated overall from pyrogenic processes.

In the atmosphere BaP degrades faster than its isomer BeP (Khedidji et al. 2013; Rabhi et al. 2018) and both of them exist overall as particulates (Magnusson et al. 2016; Liu et al. 2015), so their concentration ratio is an index of particulate emission ageing. BeP/(BaP+BeP) ratio values are ~0.5 in fresh emissions (Ladji et al. 2014). This situation occurred all-the-time through the paint premise, where the ratio ranged 0.42-0.60.

According to the set of PAHs DRs proposed by Kavouras and his coworkers (Kavouras et al. 1998), the DRs analysis was conducted on the basis of Flu/(Flu+Pyr), BaA/(BaA+Chr), BeP/(BeP+BaP) and IcdP/(IcdP+BghiP) ratios, to compare the nonsmoking and tobacco smoking zones inside the factory. Particulate PAHs found in interiors appeared as originated mostly from tobacco smoking. In fact, the Flu/(Flu+Pyr) ratio ranged 0.32÷0.37 and was similar to 0.34 determined in cigarette smoke (Table II); similarly, the BaA/(BaA+Chr) ratio ranged 0.15÷0.30 (0.19 in cigarette smoke). BeP/(BeP+BaP) ranged 0.42÷0.60 and IcdP/(IcdP+BghiP) ranged 0.35 ÷0.51, i.e., values very close to 0.64 and 0.34, respectively, consistent with tobacco smoking. These results confirm the results relative to nicotine, which was very rich in the PM_{10} samples.

3.5. Unveiling sources and correlations of PAHs through principal component analysis (PCA)

The principal component analysis (PCA) was performed in order to draw insights about the PAHs source nature in both phases, as well as to highlight links among compounds.

PCA was carried out using the statistical software (IBM, SPSS 25.0) and the Varimax rotated factor matrix method with Kaiser Normalization, based on the orthogonal rotation criterion maximizing the variance of the squared elements in the column of factors' matrix. Variables having

similar characteristics were grouped into specific factors, which indicated possible correlations between pollutants (Li et al. 2016).

The results of PCA (i.e., loading plot of 18 particulate PAHs, 13 gaseous PAHs and PCBs) are shown in Figure 8. In the loading plot (Fig. 8a), Phe, Me-Phe, Pyr and Flu, Chr, Me-Chr, Me-Flu/Pyr, and BghiF lie at the bottom of the right; meanwhile, HMW-PAHs including the BaP, BbjkaF, Pery and IcdP are located mainly at the top of the left of the graph; hence, LMW- and HMW-PAHs were sequentially separated, confirming the influence of distinct emission sources. However, a handful of PAHs, like CPPyr, Ant and BghiP showed important differences in the scattering pattern. 2- and 3-ring PAHs (2Me-Na, Me-2-Nap, Acy, Phe, Ant and diMe-Phe/Ant) belonged to one only group (Fig. 8b).

Figure 8c shows the loadings plot of naphthalene, its methylated derivatives, total particulate PAHs and PCBs for each factor extracted by PCA. Naphthalene and methyl derivatives in this score plots are grouped with particulate PAHs, while PCBs are clearly separated. This seems to suggest that an important portion of the particulate PAHs may be secondary organic aerosol, which is formed by the oxidation of LMW-PAHs (Birgul and Tasdemir 2015). By contrast, PCBs originated from a distinct emission source.

The factor analysis results are presented in Table III. Two factors were enough to explain most of the data variance. Factor 1 could explain up to 62.5% and 76.5% of the total variance for particulate) and gaseous PAHs (with strong loading of Phe, Me-Phe, Flu, Pyr, Me-Flu/Pyr, Chr, Me-Chr, BghiF and DBsumP, and 2Me-Nap, Acy, Fa, Phe, Me-Phe/Ant and DiMe-Phe/Ant, respectively). According to Li et al. (2013), Chr, Me-Chr, BkF and BbF are associated with petroleum combustion, whereas the Phe, Flu and Pyr are related to vehicular emission. On the other hand, Kulkarni and Venkataraman (2000) and Park et al. (2002) reported that Flu and Py are also originated from incineration sources, while, the 2Me-Nap, Acy and Fa (Table IV) are associated with pyrogenic sources with different combustion temperatures (Liu et al. 2015). Hence, PCA confirms what was reported in previous Section 3.4 regarding the occurrence of pyrogenic emissions in LABO and RAWM.

Factor 2 explained 28.8% and 12.6% of the total variance for particulate and gaseous PAHs (with high loading of BaA, BsumF, Pery, BaP, IcdP, BghiP, and of Nap, 1Me-Nap, 2Me-Nap, Ace and Ant, respectively).

Previous studies suggested that HMW PAHs, such as BaP, BkF, IcdP and BghiP, are suitable tracers for high temperature processes such as the burning of gasoline, diesel and biomass (Thang et al. 2019), while Nap, Ace, and Ant were associated with coal tar/coal combustion (Sofowote et al. 2008). Moreover, Kong et al. (2015) found that NaP was mainly derived from petroleum evaporation.

3.6. Partition of PAHs between particulate and gaseous phases

The concentrations of PAHs from phenanthrene to pyrene were determined both in gas and particle phase in interiors of the ENAP Company (Fig. 9). The sum of these concentrations (∑5 PAHs) in the gas phase ranged from 20 ng m^{-3} in OFFC to 75 ng m^{-3} in RAWM, with a mean of 47 ng m^{-3}, i.e., more than in the particle phase, where they ranged 1.89 (RAWM) to 5.0 ng m^{-3} (PROD) and reached a means of 2.85 ng m^{-3}.

As shown in Supplementary Information (Table SII), Phenanthrene (Phe) was found to be the most abundant in the gas phase, while methyl phenanthrene/anthracene isomers (Me-Phe/Ant) predominated in particulate phase. The important differences in the composition of gas and particle phase PAHs were consistent with the distinct source nature. Indeed, the raw materials workshop was affected by the exhaust release from traffic, while the paint production area was quite rich in particulate PAHs and probably experienced the formation of secondary particulate matter under high temperature in the presence of oxidants (Ladji et al. 2009).

In comparison with other urban and industrial sites over the world (Table V), PAHs concentrations observed in this study exceeded those measured at road traffic site in Umea, Sweden (Magnusson et al. 2016), at the ship traffic site in Venice, Italy (Gregoris et al. 2014), at the urban site in Zaragoza, Spain (Callén et al. 2008), and the background station in Gosan, Korea (Kim et al. 2012). On the other hand, PAHs concentrations were lower than those measured during the Olympic Games in Beijing, China (Ma et al. 2011) and at the industrial site of Zonguldak, Turkey (Akyuz et al. 2010).

3.7. Health risk assessment

The PM_{10}-associated and gaseous toxicity were estimated by means of the equivalent carcinogenic potency of PAHs (BaPeq). BaPeq was calculated by multiplying the mass

concentrations of each PAH compound times its corresponding toxic equivalency factor (TEFs); for this purpose, we applied the following formula (Kong et al. 2015):

$$BaPeq= 0.001*(Nap+Ace+Fa+Phe+Flu+Pyr) + 0.01*(Ant+Chr+BghiP) + + 0.1*(BaA+BbF+BkF+ IcdP) + BaP + DBA \quad (2)$$

Usually, the toxicity of ambient PAHs is calculated looking to only the particulate phase; despite that, though less carcinogenic most PAHs are emitted as vapors, and after release they partition between air and soot changing phase several times (Tasdemir and Esen 2007) depending on environmental contours.

The BaPeq rates calculated for the five sites are reported in Figure 10a. The maximum corresponded to PROD (19.7 ng m^{-3}) followed by RAWM (6.0 ng m^{-3}) for particulate PAHs, and to PROD and LABO (1.0 ng m^{-3}) for gaseous PAHs.

In the factory production area, the BaPeq daily values exceeded in both phases the maximum permissible risk level (i.e., 1 ng m^{-3}) set by the World Health Organization (WHO 2000). Moreover, the particulate phase in the atmosphere of LABO, CORR and RAWM resulted more toxic (Fig. 10a) than elsewhere in Algeria (Yassaa et al. 2001; Ladji et al. 2009).

The health risk for humans can be estimated according to exposure through inhalation (Li et al. 2016). The incremental lifetime cancer risk (ILCR) is indexed through the lifetime average daily dose (LADD) of PAHs. The equations used to estimate LADD and ILCR are:

$$LADD= C \times IR \times ED \times EF/(BW \times ALT) \quad (3)$$

$$ILCR= LADD \times CSF \quad (4)$$

Where C, instead of neat mass concentration of PAHs or PCBs (ng m^{-3}) in PM_{10} (Cetin et al. 2018; USEPA 2011), represents the sum of BaPeq of individual compounds (Jamhari et al. 2014); IR is the air inhalation rate (m^3 day^{-1}, equal to 20 for adults); ED is lifetime exposure duration (52

years for adults); EF is the exposure frequency (260 days each year excluding weekends); BW is the body weight (70 kg for adults); ALT is the average lifetime for carcinogens (70 years × 365-day year^{-1} = 25,550 days); CSF is the cancer slope factor. In this study, CSF value for BaP from inhalation is selected as 3.14 (mg kg^{-1} day^{-1}) (Chen and Liao 2006).

The average body weight of Algerian by age-specific groups are based on the National Institute of Public Health Survey September 2010 (INSP 2010).

The calculated lifetime cancer risks for this study based on the mean BaPeq and PCBs loads are shown in Figure 10b. The ILCR levels of particulate PAHs ranged from 3.6 * 10^{-5} to 9.4 * 10^{-4}, and the maximum was recorded in the production area. ILCR for gaseous PAHs were fewer, i.e., from 2.1 * 10^{-5} (at RAWM) to 4.7 * 10^{-5} (at PROD). According to them, the daily inhalation dose of particulate PAHs and cancer risk to workers in the study sites exceeded the levels of 10^{-6} to 10^{-4} proposed as acceptable by USEPA (2005), while it did not occur for gaseous PAHs.

The mean exposure levels of PCBs ranged between 2.9 * 10^{-5} at PROD to 2.0 * 10^{-3} at LABO. The mean risk level exceeded 1*10^{-3} in the laboratory and 1*10^{-4} at the office and corridor, indicating a potential health risk associated to PCBs. Cancer associated with PCBs exposure is melanoma or fight liver, gall bladder, biliary tract, gastrointestinal tract, and brain (Cetin et al. 2018). The high exposure and inhalation risk levels calculated in the laboratory can be explained with the strength of PCBs sources there.

4. Conclusion

The concentrations of n-alkanes, PAHs, PCBs and highly polar organic compounds were determined at five locations within the ENAP paint manufacturing plant during April-May 2014.

The daily concentration of PM_{10} exceeded over >60% of the period the limit value established by national Algerian and international normative, and in particular the raw material rooms were affected at important extents. Nicotine accounted for over 96% of total polar substances in the production room and corridor, its abundance inside the plant was indicative of huge tobacco smoking.

Significant differences in PAHs group distribution were found between the gas and particulate phases. Total gaseous PAHs exceeded particulate PAHs; the two phases were dominated by low

molecular weight (LMW, 2- and 3-ring compounds) and high molecular weight (HMW, 5- and 6-ring), respectively.

According to principal component analysis (PCA) and diagnostic concentration ratios, the principal sources of PAHs were identified as petroleum combustion, vehicular emission and cigarette smoke; particulate PAHs were overall associated with pyrogenic sources, while gaseous PAHs with the petrogenic ones. Secondary formation through photochemical reactions of naphthalene contributed to atmospheric particulate occurrence.

Particulate PAHs provided important contributions to the potential health risk for humans, overall in the production area. Reaching 2.0 10^{-3} and 5.2 10^{-4} at the laboratory and office, respectively, the estimated incremental lifetime cancer risk (ILCR) associated with gaseous PCBs exposure was very high compared to the maximum acceptable level comprised between 10^{-6} and 10^{-4}.

Acknowledgements The authors would like to thank the National Company of Paintings (ENAP) for their support and for providing the necessary facilities to carry out this research.

References

Akyüz M, Çabuk H. 2010. Gas–particle partitioning and seasonal variation of polycyclic aromatic hydrocarbons in the atmosphere of Zonguldak, Turkey. Science of the Total Environment 408: 5550–5558. https://doi.org/10.1016/j.scitotenv.2010.07.063

Alani R, Zhao S, Liu X, Akinrinade O, Agunbiade F, Ayejuyo O, Zhang G. 2021. Concentrations, profiles and exposure risks of polycyclic aromatic hydrocarbons (PAHs) in passive air samples from Lagos, Nigeria. Atmospheric Pollution Research 12: 101162. https://doi.org/10.1016/j.apr.2021.101162

Alves C, Nunes T, Vicente A, Gonçalves C, Evtyugina M, Marques T, Pio C, Bate-Epey F. 2014. Speciation of organic compounds in aerosols from urban background sites in the winter season. Atmospheric Research 150:57–68. https://doi.org/10.1016/j.atmosres.2014.07.012

Aquilina NJ, Havel CM, Cheung P, Harrison RM, Ho KF, Benowitz NL, Jacob III P. 2021. Ubiquitous atmospheric contamination by tobacco smoke: Nicotine and a new marker for tobacco smoke-derived particulate matter, nicotelline. Environment International 150 : 106417. https://doi.org/10.1016/j.envint.2021.106417

Birgul A, Tasdemir Y. 2015. Concentrations, Gas-Particle Partitioning, and Seasonal Variations of Polycyclic Aromatic Hydrocarbons at Four Sites in Turkey. Archives of Environmental Contamination and Toxicology 68:46–63. https://doi.org/10.1007/s00244-014-0105-8

Balducci C, Ladji R, Muto V, Romagnoli P, Yassaa N, Cecinato A. 2014. Biogenic and anthropogenic organic components of Saharan sands. Chemosphere 107:129-135. https://doi.org/10.1016/j.chemosphere.2014.02.069

Barbas B, de la Torre A, Sanz P, Navarro I, Artíñano B, Martínez MA. 2018. Gas/particle partitioning and particle size distribution of PCDD/Fs and PCBs in urban ambient air. Science of the Total Environment 624:170–179. https://doi.org/10.1016/j.scitotenv.2017.12.114

Baya MP, Bakeas EB, Sukas PA. 2004. Volatile organic compounds in the air of 25 Greek homes. Indoor and Built Environment 13:53-61. https://doi.org/10.1177/1420326X04036007

Bertoni G, Tappa R, Cecinato A. 2001. Environmental Monitoring of Semi-Volatile Polyciclic Aromatic Hydrocarbons by Means of Diffusive Sampling Devices and GC-MS Analysis. Chromatographia 53:S312-S316. https://doi.org/10.1007/BF02490348

Callén MS, de la Cruz MT, López JM, Murillo R, Navarro MV, Mastral AM. 2008. Some inferences on the mechanism of atmospheric gas/particle partitioning of polycyclic aromatic hydrocarbons (PAH) at Zaragoza (Spain). Chemosphere 73:1357–1365. https://doi.org/10.1016/j.chemosphere.2008.06.063

Can E, Özden Üzmez Ö, Döğeroğlu T, Gaga EO. 2015. Indoor air quality assessment in painting and printmaking department of a fine arts faculty building. Atmospheric Pollution Research 6:1035-1045. https://doi.org/10.1016/j.apr.2015.05.008

Cecinato A, Balducci C, Romagnoli P, Perilli M. 2014a. Behaviours of psychotropic substances in indoor and outdoor environments of Rome, Italy. Environmental Science and Pollution Research 21:9193–9200. https://doi.org/10.1007/s11356-014-2839-2

Cecinato A, Guerriero E, Balducci C, Muto V. 2014b. Use of the PAH fingerprints for identifying pollution sources. Urban Climate 10:630-643. https://doi.org/10.1016/j.uclim.2014.04.004

Cetin B, Yurdakul S, Gungormus E, Ozturk F, Sofuoglu SC. 2018. Source apportionment and carcinogenic risk assessment of passivew air sampler-derived PAHs and PCBs in a heavily industrialized region. Science of the Total Environment 633:30–41. https://doi.org/10.1016/j.scitotenv.2018.03.145

Chen CL, Kacarab M, Tang P, Cocker DR. 2016. SOA formation from naphthalene, 1-methylnaphthalene, and 2-methylnaphthalene photooxidation. Atmospheric Environment 131:424-433. https://doi.org/10.1016/j.atmosenv.2016.02.007

Chen SC, Liao CM. 2006. Health risk assessment on human exposed to environmental polycyclic aromatic hydrocarbons pollution sources. Science of the Total Environment 366:112-123. https://doi.org/10.1016/j.scitotenv.2005.08.047

Colombo A, Benfenati E, Bugatti SG, Lodi M, Mariani A, Musmeci L, Rotella G, Senese V, Ziemacki G, Fanelli R. 2013. PCDD/Fs and PCBs in ambient air in a highly industrialized city in Northern Italy. Chemosphere 90:2352–2357. https://doi.org/10.1016/j.chemosphere.2012.10.025

Directive 2008/50/EC of the European Parliament and of the Council of 21 May 2008 on ambient air quality and cleaner air for Europe 152:1–44.

Dobbins RA, Fletcher RA, Benner BA, Hoeft S. 2006. Polycyclic aromatic hydrocarbons in flames, in diesel fuels, an in diesel emissions. Combustion and Flame 144:773–781. https://doi.org/10.1016/j.combustflame.2005.09.008

Eatough DJ, Benner CK, Tang H, Landon V, Richards G, Caka FM, Crawford J, Lewis EA, Haasen LD, Eatough NL. 1989. The chemical composition of ETS III: identification of conservative tracers of ETS. Environment International 15:19–28. https://doi.org/10.1016/0160-4120(89)90005-6

Feliu A, Fu M , Russo M, Martinez C, Sureda X, José López M, Cortés N, Fernández E. 2020. Exposure to second-hand tobacco smoke in waterpipe cafés in Barcelona, Spain: An assessment of airborne nicotine and PM2.5. Environmental Research 184:109347. https://doi.org/10.1016/j.envres.2020.109347

Fromme H, Sysoltseva M, Achten C, Bühl T, Röhl C, Leubner S, Gerull F, Gessner A, Kraft M, Burghardt R, Schober W, Völkel W. 2023. Polycyclic aromatic hydrocarbons including dibenzopyrenes in indoor air samples from schools and residences in Germany. Atmospheric Environment 309:119946. https://doi.org/10.1016/j.atmosenv.2023.119946

Gao DW, Wen ZD. 2016. Phthalate esters in the environment: a critical review of their occurrence, biodegradation, and removal during wastewater treatment processes. Science of the Total Environment 541:986–1001. https://doi.org/10.1016/j.scitotenv.2015.09.148

Gheriani A, Boudehane A, Lounas A, Balducci C, Cecinato A, Khadraoui A. 2022. n-Alkanes and Polycyclic Aromatic Hydrocarbons in Deposition Dust and PM10 of Interiors in Touggourt Region, Algeria. Archives of Environmental Contamination and Toxicology 83:26–241. https://doi.org/10.1007/s00244-022-00954-3

Ghobakhloo S, Khoshakhlagh AH, Morais S, Tehrani AM. 2023. Exposure to Volatile Organic Compounds in Paint Production Plants: Levels and Potential Human Health Risks. Toxics 11 (2) 111. https://doi.org/10.3390/toxics11020111

Gregoris E, Argiriadis E, Vecchiato M, Zambon S, De Pieri S, Donateo A, Contini D, Piazza R, Barbante C, Gambaro A. 2014. Gas-particle distributions, sources and health effects of

polycyclic aromatic hydrocarbons (PAHs), polychlorinated biphenyls (PCBs) and polychlorinated naphthalenes (PCNs) in Venice aerosols. Science of the Total Environment 476-477:393-405. https://doi.org/10.1016/j.scitotenv.2014.01.036

Henderson E, Guerrero LAR, Continente X, Fernández E, Tigova O, Cortés-Francisco N, Semple S, Dobson R, Tzortzi A, Vyzikidou VK, Gorini G, Geshanova G, Mons U, Przewozniak K, Precioso J, Brad R, López MJ. 2023. Measurement of airborne nicotine, as a marker of secondhand smoke exposure, in homes with residents who smoke in 9 European countries. Environmental Research 219: 115118. https://doi.org/10.1016/j.envres.2022.115118

Hu H, Tian M, Zhang L, Yang F, Peng C, Chen Y, Shi G, Yao X, Jiang C, Wang J. 2019. Sources and gas-particle partitioning of atmospheric parent, oxygenated, and nitrated polycyclic aromatic hydrocarbons in a humid city in southwest China. Atmospheric Environment S1352-2310(19)30145-1. https://doi.org/10.1016/j.atmosenv.2019.02.041

INSP. 2010. Transition épidémiologique et système de santé Projet TAHINA. L'Obésité chez l'adulte de 35 à 70 ans en Algérie. Contrat n° ICA3-CT-2002-10011. Institut National de Santé Publique, Algérie.

Jamhari AA, Sahani M, Latif MT, Chan KM, Tan HS, Khan MF, Tahir NM. 2014. Concentration and source identification of polycyclic aromatic hydrocarbons (PAHs) in PM10 of urban, industrial and semi-urban areas in Malaysia. Atmospheric Environment 86:16–27. https://doi.org/10.1016/j.atmosenv.2013.12.019

Kautzman KE, Surratt JD, Chan MN, Chan AWH, Hersey SP, Chhabra PS, Dalleska NF, Wennberg PO, Flagan RC, Seinfeld JH. 2010. Chemical composition of gas- and aerosol-phase products from the photooxidation of naphthalene. Journal of Physical Chemistry A 114:913-934. http://doi.org/10.1021/jp908530s

Kavouras IG, Stratigakis N, Stephanou EG. 1998. Iso- and anteisoalkanes: specific tracers of environmental tobacco smoke in indoor and outdoor particle-size distributed urban aerosols. Environmental Science and Technology 32:1369-1377. https://doi.org/10.1021/es970634e

Kermani M, Taghizadeh F, Jafari AJ, Gholami M, Shahsavani A, Nakhjirgan P. 2023. PAHs pollution in the outdoor air of areas with various land uses in the industrial city of Iran: distribution,

source apportionment, and risk assessment. Heliyon 9:e17357. https://doi.org/10.1016/j.heliyon.2023.e17357

Khedidji S, Ladji R, Yassaa N. 2013. A wintertime study of polycyclic aromatic hydrocarbons (PAHs) in indoor and outdoor air in a big student residence in Algiers, Algeria. Environmental Science and Pollution Research. 20:4906–4919. https://doi.org/10.1007/s11356-012-1430-y

Khedidji S, Balducci C, Ladji R, Cecinato A, Perilli M, Yassaa N. 2017a. Chemical composition of particulate organic matter at industrial, university and forest areas located in Bouira province, Algeria. Atmospheric Pollution Research 8:474-482. https://doi.org/10.1016/j.apr.2016.12.005

Khedidji S, Croes K, Yassaa N, Ladji R, Denison MS, Baeyens W, Elskens M. 2017b. Assessment of dioxin-like activity in PM10 air samples from an industrial location in Algeria, using the DRE-CALUX bioassay. Environmental Science and Pollution Research 24:11868–11877. https://doi.org/10.1007/s11356-015-5841-4

Khedidji S, Konrad M, Rabhi L, Spindler G, Fomba KW, Van Pinxteren D, Yassaa N, Herrmann H. 2020. Chemical Characterization of Marine Aerosols in a South Mediterranean Coastal Area Located in Bou Ismaïl, Algeria. Aerosol and Air Quality Research 20: 2448–2473 https://doi.org/10.4209/aaqr.2019.09.0458

Khoshakhlagh AH, Yazdanirad S, Saberi HR, Pao-Chi Liao PC. 2023a. Health risk assessment of exposure to various vapors and fumes in a factory of automobile manufacturing. Heliyon 9:e18583. https://doi.org/10.1016/j.heliyon.2023.e18583

Khoshakhlagh AH, Chuang KJ, Kumar P. 2023b. Health risk assessment of exposure to ambient formaldehyde in carpet manufacturing industries. Environmental Science and Pollution Research 30:16386–16397. https://doi.org/10.1007/s11356-022-23353-6

Kim JY, Lee JY, Choi SD, Kim YP, Ghim YS. 2012. Gaseous and particulate polycyclic aromatic hydrocarbons at the Gosan background site in East Asia. Atmospheric Environment 49:311-319. https://doi.org/10.1016/j.atmosenv.2011.11.029

Kim KH, Jahan SA, Kabir E, Brown RJC. 2013. A review of airborne polycyclic aromatic hydrocarbons (PAHs) and their human health effects. Environment International 60:71-80. https://doi.org/10.1016/j.envint.2013.07.019

Kong S, Li X, Li L, Yin Y, Chen K, Yuan L, Zhang Y, Shan Y, Ji Y. 2015. Variation of polycyclic aromatic hydrocarbons in atmospheric PM2.5 during winter haze period around 2014 Chinese Spring Festival at Nanjing: Insights of source changes, air mass direction and firework particle injection. Science of the Total Environment 520:59-72. https://doi.org/10.1016/j.scitotenv.2015.03.001

Kulkarni P, Venkataraman C. 2000. Atmospheric polycyclic aromatic hydrocarbons in Mumbai, India. Atmospheric Environment 34:2785–2790. https://doi.org/10.1016/S1352-2310(99)00312-X

Ladji R, Yassaa N, Balducci C, Cecinato A, Meklati BY. 2009. Distribution of the solvent-extractable organic compounds in fine (PM1) and coarse (PM1-10) particles in urban, industrial and forest atmospheres of Northern Algeria. Science of the Total Environment 408:415-424. https://doi.org/10.1016/j.scitotenv.2009.09.033

Ladji R, Yassaa N, Balducci C, Cecinato A. 2014. Particle size distribution of nalkanes and polycyclic aromatic hydrocarbons (PAHS) in urban and industrial aerosol of Algiers, Algeria. Environmental Science and Pollution Research 21:1819-1832. https://doi.org/10.1007/s11356-013-2074-2

Li X, Wang Y, Guo X, Wang Y. 2013. Seasonal variation and source apportionment of organic and inorganic compounds in PM2.5 and PM10 particulates in Beijing, China. Journal of Environmental Sciences 25(4):741-750. https://doi.org/10.1016/S1001-0742(12)60121-1

Li X, Kong S, Yin Y, Li L, Yuan L, Li Q, Xiao H, Chen K. 2016. Polycyclic aromatic hydrocarbons (PAHs) in atmospheric PM2.5 around 2013 Asian Youth Games period in Nanjing. Atmospheric Research 174:85-96. https://doi.org/10.1016/j.atmosres.2016.01.010

Liu Y, Gao Y, Yua N, Zhang C, Wang S, Ma L, Zhao J, Lohmann R. 2015. Particulate matter, gaseous and particulate polycyclic aromatic hydrocarbons (PAHs) in an urban traffic tunnel of China: Emission from on-road vehicles and gas-particle partitioning. Chemosphere 134:52–59. https://doi.org/10.1016/j.chemosphere.2015.03.065

Lu R, Wu J, Turco RP, Winer AM, Atkinson R, Arey J, Paulson SE, Lurmann FW, Miguel AH, Eiguren-Fernandez A. 2005. Naphthalene distributions and human exposure in southern

California. Atmospheric Environment 39:489-507. https://doi.org/10.1016/j.atmosenv.2004.09.045

Ma WL, Sun DZ, Shen WG, Yang M, Qi H, Liu LY, Shen JM, Li YF. 2011. Atmospheric concentrations, sources and gas-particle partitioning of PAHs in Beijing after the 29th Olympic Games. Environmental Pollution 159:1794-1801. https://doi.org/10.1016/j.envpol.2011.03.025

Magnusson R, Arnoldsson K, Lejon C, Hägglund L, Wingfors H. 2016. Field evaluation and calibration of a small axial passive air sampler for gaseous and particle bound polycyclic aromatic hydrocarbons (PAHs) and oxygenated PAHs. Environmental Pollution 216:235-244. https://doi.org/10.1016/j.envpol.2016.05.067

Morawska L, Zhang J. 2002. Combustion sources of particles. 1. Health relevance and source signatures. Chemosphere 49:1045–1058. https://doi.org/10.1016/S0045-6535(02)00241-2

Mostert MMR, Ayoko GA, Kokot S. 2010. Application of chemometrics to analysis of soil pollutants. TrAC Trends in Analytical Chemistry 29:430-445. https://doi.org/10.1016/j.trac.2010.02.009

Moussaoui Y, Tuduri L, Kerchich Y, Meklati BY, Eppe G. 2012. Atmospheric concentrations of PCDD/Fs, dl-PCBs and some pesticides in northern Algeria using passive air sampling. Chemosphere 88:270–277. http://doi.org/10.1016/j.chemosphere.2012.02.025

Nadali A, Leili M, Bahrami A, Karami M, Afkhami A. 2021. Phase distribution and risk assessment of PAHs in ambient air of Hamadan, Iran. Ecotoxicology and Environmental Safety 209:111807. https://doi.org/10.1016/j.ecoenv.2020.111807

Nishino N, Arey J, Atkinson R. 2012. 2-Formylcinnamaldehyde formation yield from the OH radical-initiated reaction of naphthalene: effect of NO (2) concentration. Environmental Science and Technology 46:8198-8204. http://doi.org/10.1021/es301865t

Ohura T, Amagai T, Shen X, Li S, Zhang P, Zhu L. 2009. Comparative study on indoor air quality in Japan and China: characteristics of residential indoor and outdoor VOCs. Atmospheric Environment 43:6352-6359. https://doi.org/10.1016/j.atmosenv.2009.09.022

Pandey SK, Kim KH, Brown RJC. 2011. A review of techniques for the determination of polycyclic aromatic hydrocarbons in air. TrAC Trends in Analytical Chemistry 30(11):1716-1739. https://doi.org/10.1016/j.trac.2011.06.017

Park SS, Kim YJ, Kang CH. 2002. Atmospheric polycyclic aromatic hydrocarbons in Seoul, Korea. Atmospheric Environment 36:2917–2924. https://doi.org/10.1016/S1352-2310(02)00206-6

PDRA-ED. 2006. Executive Decree No 06–02 of 07 January 2006, page 3, defining value limits, alert thresholds and air quality objectives in case of atmospheric pollution in Algeria (in French). People's Democratic Republic of Algeria, Algeria.

Rabhi L, Lemou A, Cecinato A, Balducci C, Cherifi N, Ladji R, Yassaa N. 2018. Polycyclic aromatic hydrocarbons, phthalates, parabens and other environmental contaminants in dust and suspended particulates of Algiers, Algeria. Environmental Science and Pollution Research 25:24253–24265. https://doi.org/10.1007/s11356-018-2496-y

Romagnoli P, Balducci C, Perilli M, Gherardi M, Gordiani AC, Gariazzo C, Gatto MP, Cecinato A. 2014. Indoor PAHs at schools, homes and offices in Rome, Italy. Atmospheric Environment 92:51-59. https://doi.org/10.1016/j.atmosenv.2014.03.063

Romagnoli P, Balducci C, Perilli M, Esposito G, Cecinato A. 2019. Organic molecular markers in marine aerosols over the Western Mediterranean Sea. Environment Pollution 248:145-158. https://doi.org/10.1016/j.envpol.2019.02.020

Rostami R, Zarei A, Saranjam B, Ghaffari HR, Hazrati S, Poureshg Y, Fazlzade M. 2019. Exposure and risk assessment of PAHs in indoor air of waterpipe cafés in Ardebil, Iran. Building and Environment 155:47-57. https://doi.org/10.1016/j.buildenv.2019.03.031

Sarti E, Pasti L, Scaroni I, Casali P, Cavazzini A, Rossi M. 2017. Determination of n-alkanes, PAHs and nitro-PAHs in PM2.5 and PM1 sampled in the surroundings of a municipal waste incinerator. Atmospheric Environment 149:12–23. https://doi.org/10.1016/j.atmosenv.2016.11.016

Sofowote UM, McCarry BE, Marvin CH. 2008. Source apportionment of PAH in Hamilton Harbour suspended sediments: comparison of two factor analysis methods. Environmental Science and Technology 42(16):6007-6014. https://doi.org/10.1021/es800219z

Tasdemir Y, Esen F. 2007. Urban air PAHs: concentrations, temporal changes and gas/particle partitioning at a traffic site in Turkey. Atmospheric Research 84:1-12. https://doi.org/10.1016/j.atmosres.2006.04.003

Thang PQ, Kim SJ, Lee SJ, Ye J, Seo YK, Baeke SO, Choi SD. 2019. Seasonal characteristics of particulate polycyclic aromatic hydrocarbons (PAHs) in a petrochemical and oil refinery industrial area on the west coast of South Korea. Atmospheric Environment 198:398-406. https://doi.org/10.1016/j.atmosenv.2018.11.008

Tobiszewski M, Namiesnik J. 2012. PAH diagnostic ratios for the identification of pollution emission sources. Environment Pollution 162:110-119. http://doi.org/10.1016/j.envpol.2011.10.025

Torrey, CM, Moon KA, Williams DAL, Green T, Cohen JE, Navas-Acien A, Breysse PN. 2015. Waterpipe cafes in Baltimore, Maryland: carbon monoxide, particulate matter, and nicotine exposure. Journal of exposure science and environmental epidemiology 25:405–410. https://doi.org/10.1038/jes.2014.19

Tran TM, Kannan K. 2015. Occurrence of phthalate diesters in particulate and vapor phases in indoor air and implications for human exposure in Albany, New York, USA. Archives of Environmental Contamination and Toxicology 68:489–499. https://doi.org/10.1007/s00244-015-0140-0

Valle-Hernández BL, López-bello E, Torres-Rodríguez M, Agapito-Abraham C, Mugica-Álvarez V. 2021. Preliminary study of soot and polycyclic aromatic hydrocarbons in emitted particles from adobe kilns that use scrap tires as fuel. Atmósfera 34:41-57. https://doi.org/10.20937/ATM.52756

USEPA. 2005. Guidelines for Carcinogenic Risk Assessment. United States Environmental Protection Agency, Washington, USA.

USEPA. 2011. Exposure Factors Handbook, EPA/600/R-090/052F. Office of Research and Development National Center for Environmental Assessment. United States Environmental Protection Agency, Washington, USA.

Wei C, Han Y, Musa Bandowe BA, Cao J, Huang R, Ni H, Tian J, Wilcke W. 2015. Occurrence, gas/particle partitioning and carcinogenic risk of polycyclic aromatic hydrocarbons and their oxygen and nitrogen containing derivatives in Xi'an, central China. Science of the Total Environment 505:814–822. https://doi.org/10.1016/j.scitotenv.2014.10.054

WHO. 2021. World Health Statistics 2021: Monitoring Health for the SDGs, Sustainable Development Goals. World Health Organization, Geneva, Switzerland.

WHO. 2000. Air Quality Guidelines for Europe, Second Edition. World Health Organization, Geneva, Switzerland.

Wu Y, Yang L, Zheng X, Zhang S, Song S, Li J, Hao J. 2014. Characterization and source apportionment of particulate PAHs in the roadside environment in Beijing. Science of the Total Environment 470-471(2):76-83. https://doi.org/10.1016/j.scitotenv.2013.09.066

Yassaa N, Meklati BY, Cecinato A, Marino F. 2001. Particulate n-alkanes, n-alkanoic acids and polycyclic aromatic hydrocarbons in the atmosphere of Algiers City Area. Atmospheric Environment 35:1843-1851. https://doi.org/10.1016/S1352-2310(00)00514-8

Yassaa N, Cecinato A. 2005. Composition of torched crude oil organic particulate emitted by refinery and its similarity to atmospheric aerosol in the surrounding area. Chemosphere 60:1660-1666. https://doi.org/10.1016/j.chemosphere.2005.02.041

Yenisoy-Karakaş S, Öz M, Gaga EO. 2012. Seasonal variation, sources, and gas/particle concentrations of PCBs and OCPs at high altitude suburban site in Western Black Sea Region of Turkey. Journal of Environmental Management 14(5):1365-1374. https://doi.org/10.1039/c2em30038a

Zakaria MP, Takada H, Tsutsumi S, Ohno K, Yamada J, Kouno E, Kumata H. 2002. Distribution of polycyclic aromatic hydrocarbons (PAHs) in rivers and estuaries in Malaysia: a widespread input of petrogenic PAHs. Environmental Science and Technology 36:1907–1918. https://doi.org/10.1021/es011278+

Zhang W, Zhang S, Wan C, Yue D, Ye Y, Wang X. 2008. Source diagnostics of polycyclic aromatic hydrocarbons in urban road runoff, dust, rain and canopy through fall. Environment Pollution 153:594-601. https://doi.org/10.1016/j.envpol.2007.09.004

Zhang B, Haji F, Kaufman P, Muir S, Ferrence R. 2015. Enter at your own risk": a multimethod study of air quality and biological measures in Canadian waterpipe cafes. Tobacco Control 24:175–181. https://doi.org/10.1136/tobaccocontrol-2013-051180

Table Headings:

Table I. Mean suspended particle concentrations (PM_{10}) and component loads at the study

Table II**.** Diagnostic ratios calculated for gas and particle phase air samples in this study

Table III. Factor loadings of particulates PAHs in the PCA analysis. Entries in bold indicate high factor loading

Table IV. Factor loadings of gaseous PAHs in the PCA analysis. Entries in bold indicate high factor loading

Table V. Average gas and particulate PAHs (ng m^{-3}) measured in this study and in recent literature data.

Table I. Mean suspended particle concentrations (PM_{10}) and component loads at the study locations.

Site	PROD	LABO	OFFC	CORR	RAWM
PM_{10} (µg m^{-3})	46.7	55.8	42.0	58.8	95.2
∑ PAHs (gaseous, ng m^{-3})	2 329	1 946	1 797	1 507	834
∑ PAHs (particulate, ng m^{-3})	34.7	16.3	7.0	15.4	12.8
∑ alkanes (particulate, ng m^{-3})	484	477	201	306	114
∑ HPOC (particulate, ng m^{-3})	424	185	147	240	156
PCBs (gaseous, ng m^{-3})	0.6	42.4	10.9	3.2	1.1

Table II. Diagnostic ratios calculated for gas and particle phase air samples in this study.

Ratios	Phases	PROD	LABO	OFFC	CORR	RAWM
Ant/(Phe+Ant)	*particle*	0.41	0.43	0.37	0.53	0.51
	gas	0.06	0.07	0.05	0.06	0.08
Flu/(Flu+Pyr)	*particle*	0.32	0.33	0.37	0.33	0.35
	gas	0.62	0.64	0.65	0.58	0.62
alkylate PAHs/parent PAHs	*Particle(Chr/Me-Chr)*	1.43	1.27	1.29	1.48	1.57
	gas (Nap/Me-Nap)	0.64	1.07	0.53	0.88	1.02
BeP/(BeP+BaP)	*Particle*	0.60	0.55	0.54	0.42	0.58
	gas	n.d.	n.d.	n.d.	n.d.	n.d.
BaA/(BaA+Chr)	*Particle*	0.15	0.22	0.21	0.30	0.21
	gas	n.d.	n.d.	n.d.	n.d.	n.d.
IcdP/(BghiP+IcdP)	*particle*	0.37	0.40	0.38	0.51	0.35
	gas	n.d.	n.d.	n.d.	n.d.	n.d.

n.d. not detected

Table III. Factor loadings of particulates PAHs in the PCA analysis. Entries in bold indicate high factor loading.

PAHs (Particle)	PC Component 1	PC Component 2
Phe	**0.979**	0.141
Ant	0.685	0.545
MePhe	**0.973**	0.033
Flu	**0.988**	0.018
Pyr	**0.976**	0.122
MeFluPyr	**0.833**	0.381
BcPhe	0.637	0.769
BaA	0.416	**0.901**
Chr	**0.940**	0.340
MeChr	**0.915**	0.355
BghiF	**0.882**	0.409
CPPyr	0.407	0.571
BsumF	0.056	**0.978**
Pery	-0.088	**0.982**
BeP	0.626	0.775
BaP	-0.054	**0.98**
DBahA	-0.87	0.41
IcdP	-0.159	**0.96**
BghiP	0.31	**0.94**
DBsumP	**0.81**	-0.103
Initial % of variance	62.5	28.8
Cumulative %	62.5	91.3
Sources	Petroleum, vehicular	biomass combustion

Table IV. Factor loadings of gaseous PAHs in the PCA analysis. Entries in bold indicate high factor loading.

PAHs (gas)	PC Component 1	PC Component 2
Nap	-0.089	**0.86**
1-Me Nap	0.44	**0.87**
2-Me Nap	0.65	**0.74**
Me-2-Nap	**0.71**	0.69
Acy	**0.87**	0.42
Ace	0.30	**0.90**
Fa	**0.96**	0.106
Phe	**0.82**	0.57
Ant	0.66	**0.72**
Me-Phe/Ant	**0.99**	0.096
DiMe-Phe/Ant	**0.77**	0.62
Flu	0.62	0.61
Pyr	0.43	0.57
Initial % of variance	76.5	12.6
Cumulative %	76.5	89.2
Sources	pyrogenic	petroleum combustion

Table V. Average gas and particulate PAHs (ng m^{-3}) measured in this study and in recent literature data.

Sampling sites		Lakhdaria, Algeria	Umea, Sweden	Venice, Italy	Venice, Italy	Beijing, China	Zonguldak, Turkey	Zaragoza, Spain	Gosan, Korea
Feature		industry	road traffic	ship traffic	ship traffic	Olympic Games	industry	urban	background
Period		2014-15	2014	2012	2009	2008	2007-08	2003-04	2001-03
PHE	G	39.1	1.2	0.86	1.6	43.1	106	2.2	0.55
	P	0.38	0.068	0.025	0.034	4.6	10.9	0.129	0.324
ANT	G	2.44	0.11	0.023	0.034	7.3	26.2	0.45	0.031
	P	0.29	0.019	0.0025	0.003	0.5	4.6	n.d.	0.009
Me-PHE/ANT	G	8.6	0.038	n.e.	n.e.	n.e.	n.e.	2.17	n.e.
	P	1.48	0.01	n.e.	n.e.	n.e.	n.e.	0.079	n.e.
FLU	G	1.90	0.094	0.056	0.97	15.2	37.4	0.84	0.21
	P	0.31	0.13	0.044	0.68	12.3	31.8	0.23	0.53
PYR	G	1.18	0.073	0.05	0.65	9.9	36.1	0.82	0.207
	P	0.62	0.13	0.051	0.46	10.5	24.9	0.31	0.36
Ref.			a	b	b	c	d	e	f

Symbols: G = gas phase; P = particulate phase; n.e. not examined; n.d. not detected

References: a) Magnusson et al., 2016; b) Gregoris et al., 2014; c) Ma et al., 2011; d) Akyuz et al., 2010; e) Callén et al., 2008; f) Kim et al., 2012.

Figures captions:

Fig. 1. Map of sampling locations inside the ENAP estate of Lakhdaria.

Fig. 2. PM_{10} concentrations (μg m^{-3}) measured in different micro-environments inside the national company of paintings (ENAP).

Fig. 3. *n*-Alkanes distributions in particulate atmospheric deposition collected in different microenvironments in the ENAP and inside the building (ng m^{-3}).

Fig. 4. The distributions of individual PAHs in particulate atmospheric deposition collected in different microenvironments in the ENAP and inside the building (ng m^{-3}).

Fig. 5. The distributions of individual polar compounds in particulate atmospheric deposition collected in different microenvironments in the ENAP and inside the building (ng m^{-3}).

Fig. 6. The distributions of individual PAHs in gaseous atmospheric deposition collected in different microenvironments in the ENAP and inside the building (ng m^{-3}).

Fig. 7. Benzene ring number distribution of PAHs (a) gaseous and (b) particulate phase measured in five sites located inside ENAP.

Fig. 8. Principal component analysis as loading plot of (a) 18 particulate PAHs; (b) 13 gaseous PAHs; (c) naphthalene, NAPH methylated derivatives, total particulate PAHs and PCBs, measured inside the company.

Fig. 9. Concentrations of 5 PAHs compounds in particulate and gaseous phases measured in five interiors of ENAP.

Fig. 10. BaP equivalent (BaPeq) concentrations and incremental lifetime cancer risk (ILCR) measured at the five sites inside the factory.

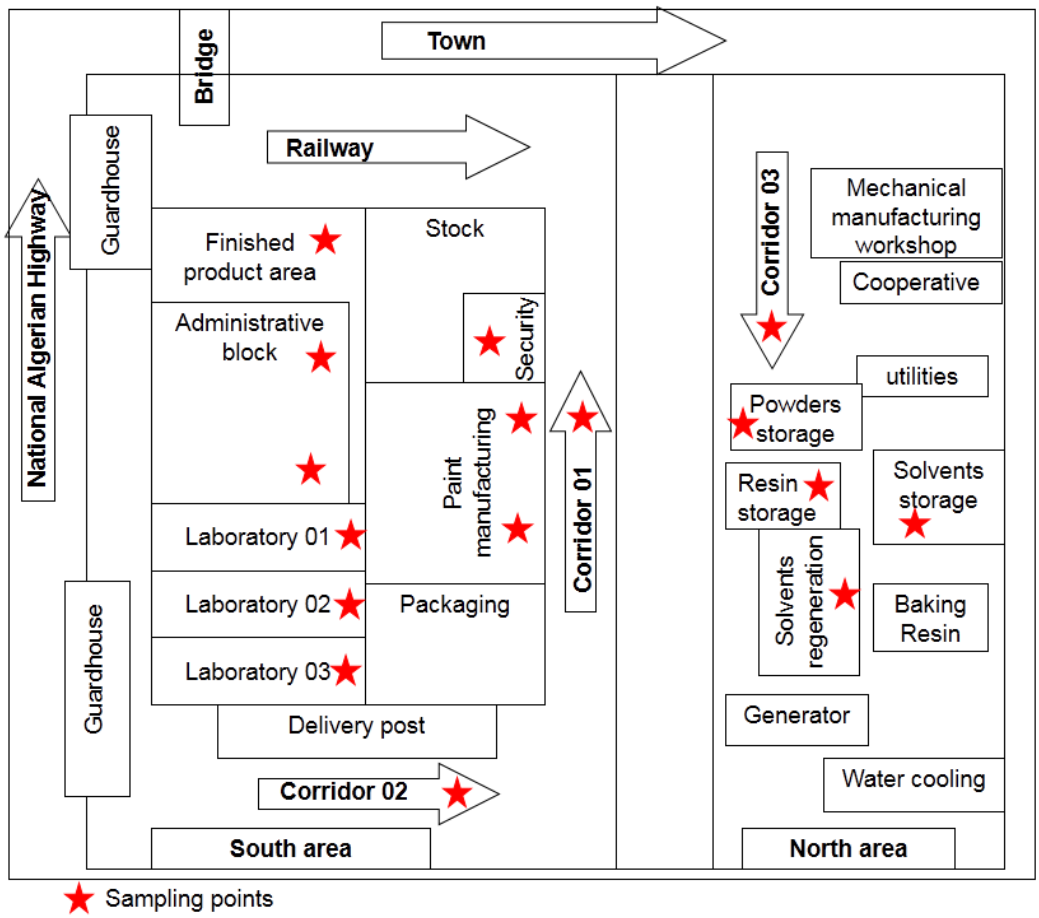

Fig. 1. Map of sampling locations inside the ENAP estate of Lakhdaria.

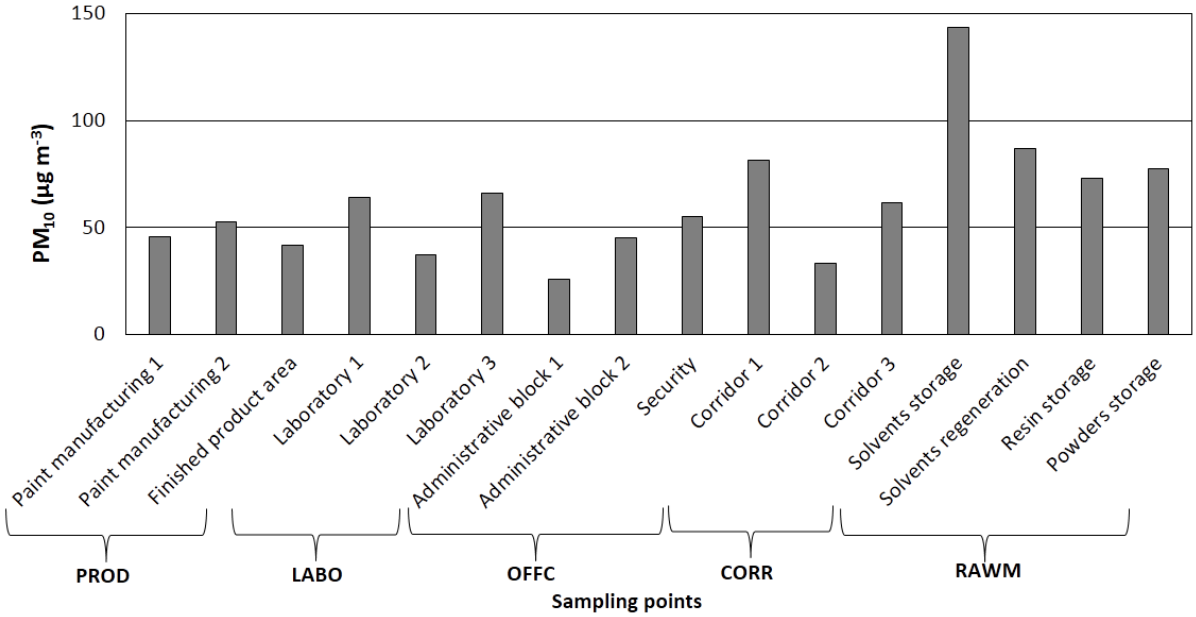

Fig. 2. PM_{10} concentrations (µg m^{-3}) measured in different micro-environments inside the national company of paintings (ENAP).

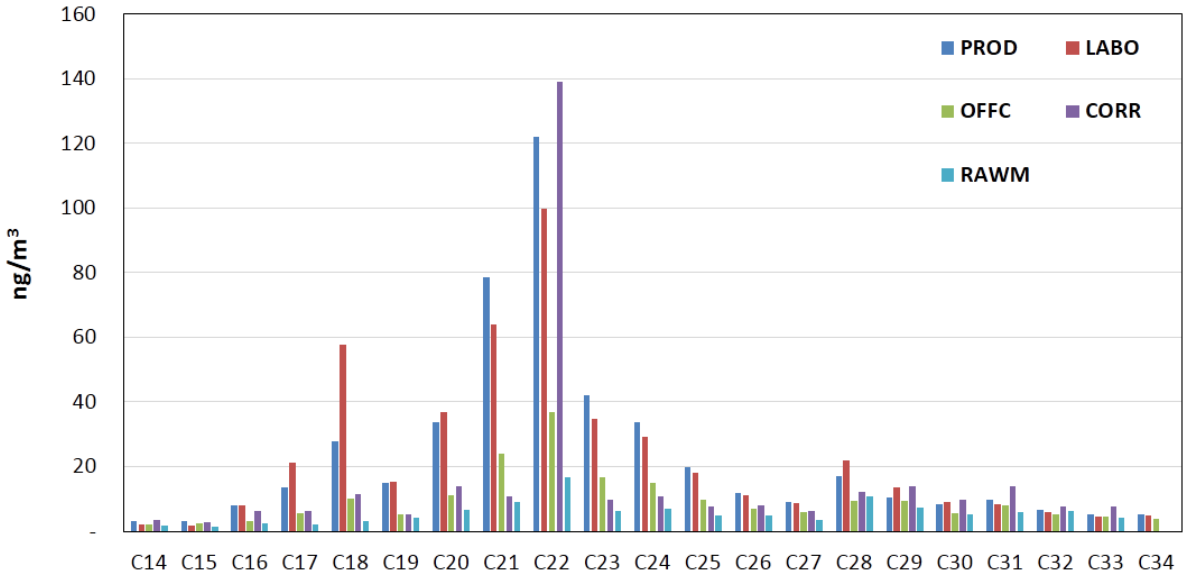

Fig. 3. n-Alkanes distributions in particulate atmospheric deposition collected in different microenvironments in the ENAP and inside the building (ng m^{-3}).

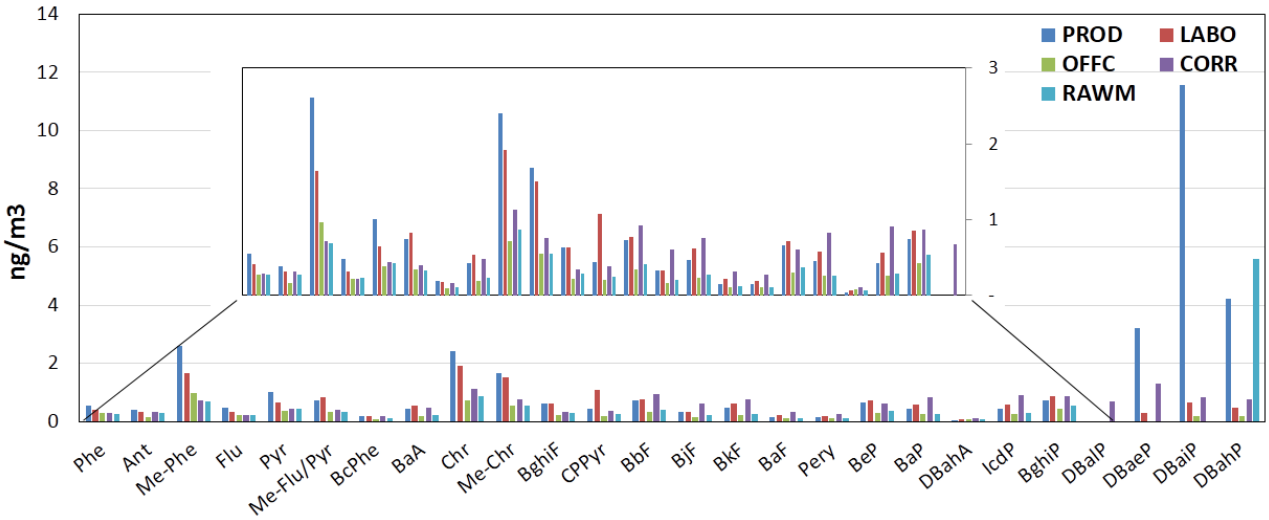

Fig. 4. The distributions of individual PAHs in particulate atmospheric deposition collected in different microenvironments in the ENAP and inside the building (ng m^{-3}).

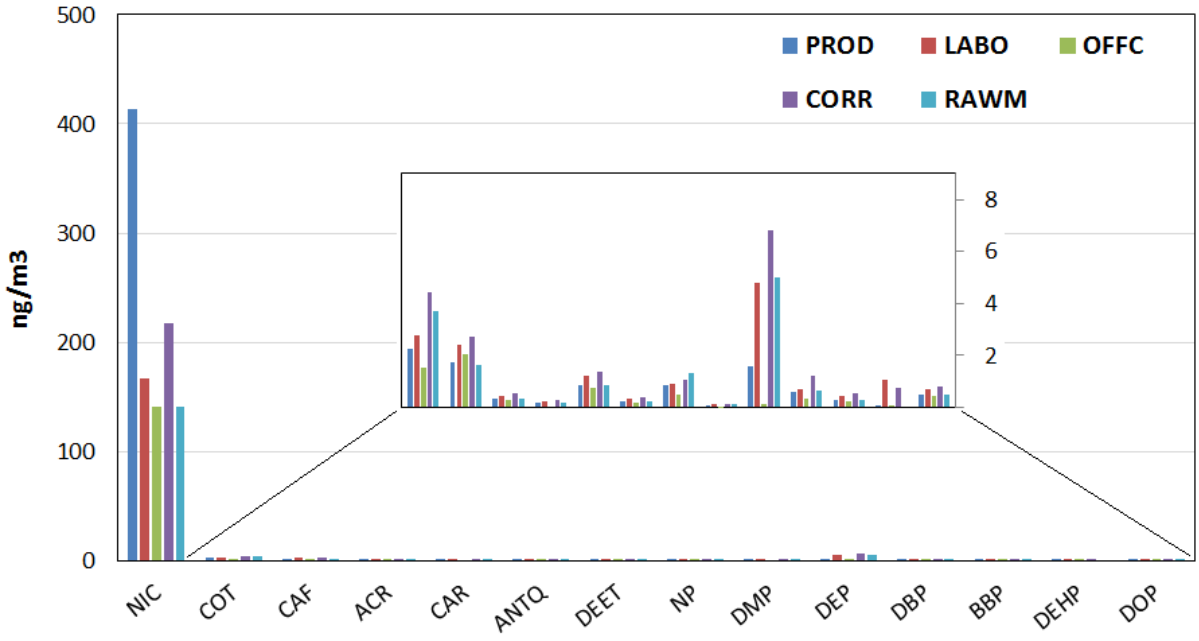

Fig. 5. The distributions of individual polar compounds in particulate atmospheric deposition collected in different microenvironments in the ENAP and inside the building (ng m^{-3}).

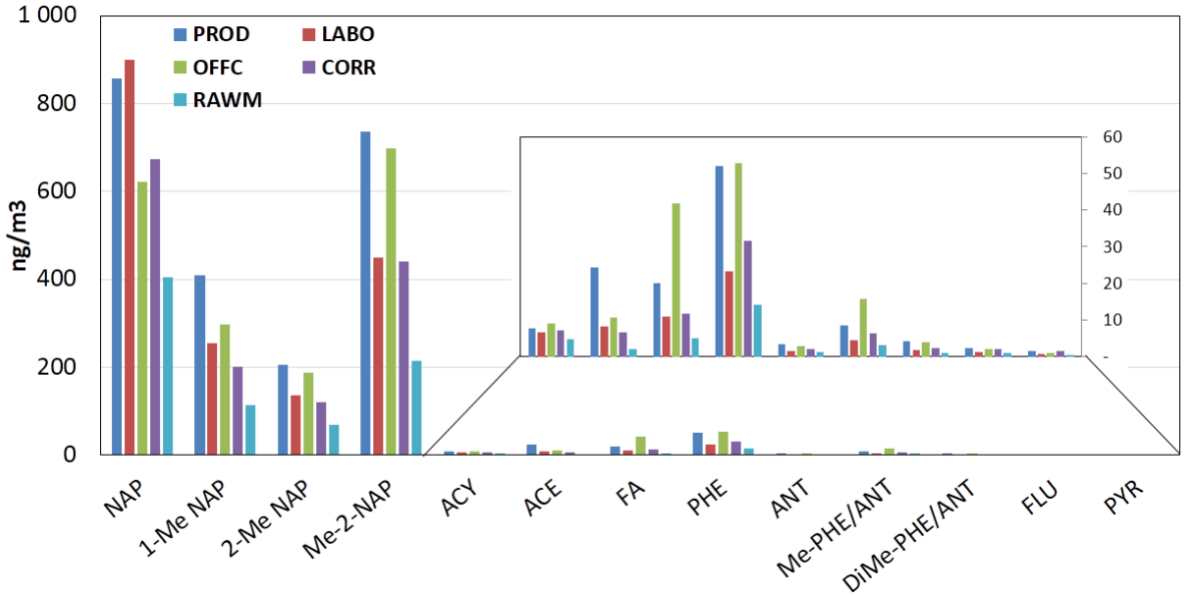

Fig. 6. The distributions of individual PAHs in gaseous atmospheric deposition collected in different microenvironments in the ENAP and inside the building (ng m^{-3}).

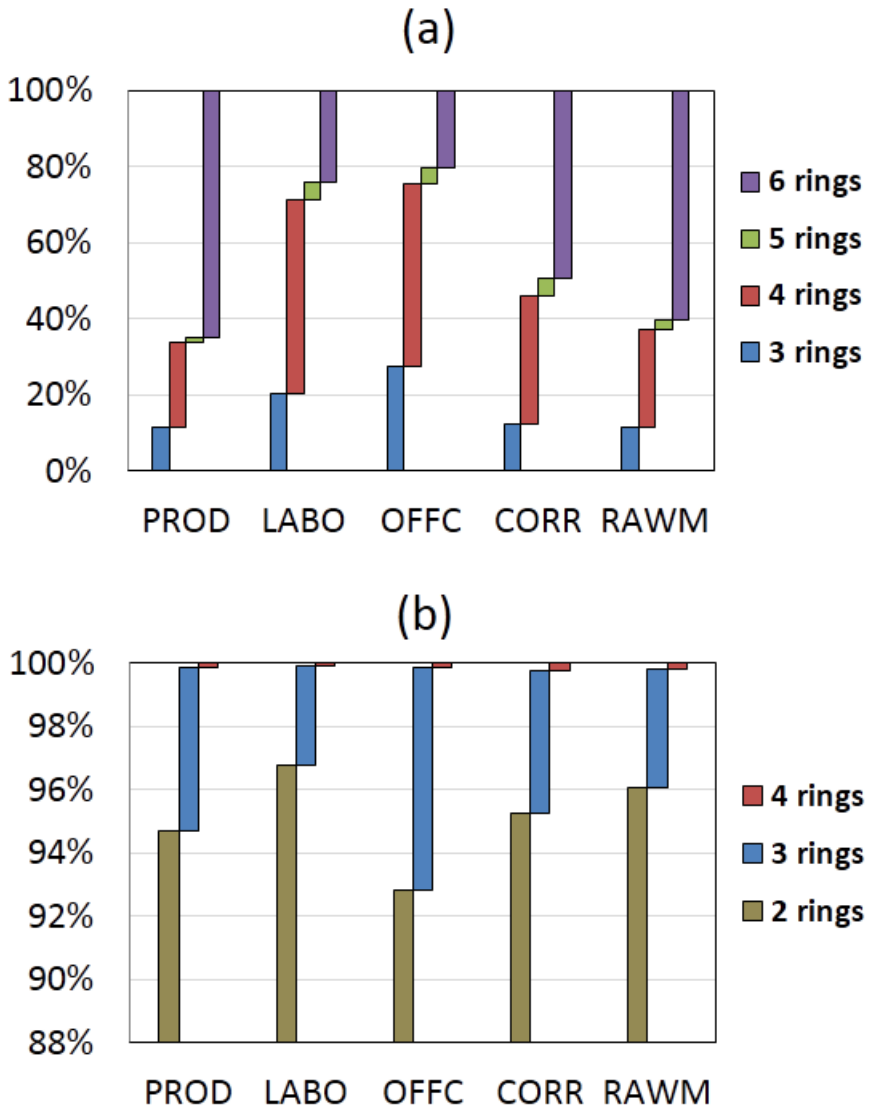

Fig. 7. Benzene ring number distribution of PAHs (a) gaseous and (b) particulate phase measured in five sites located inside ENAP.

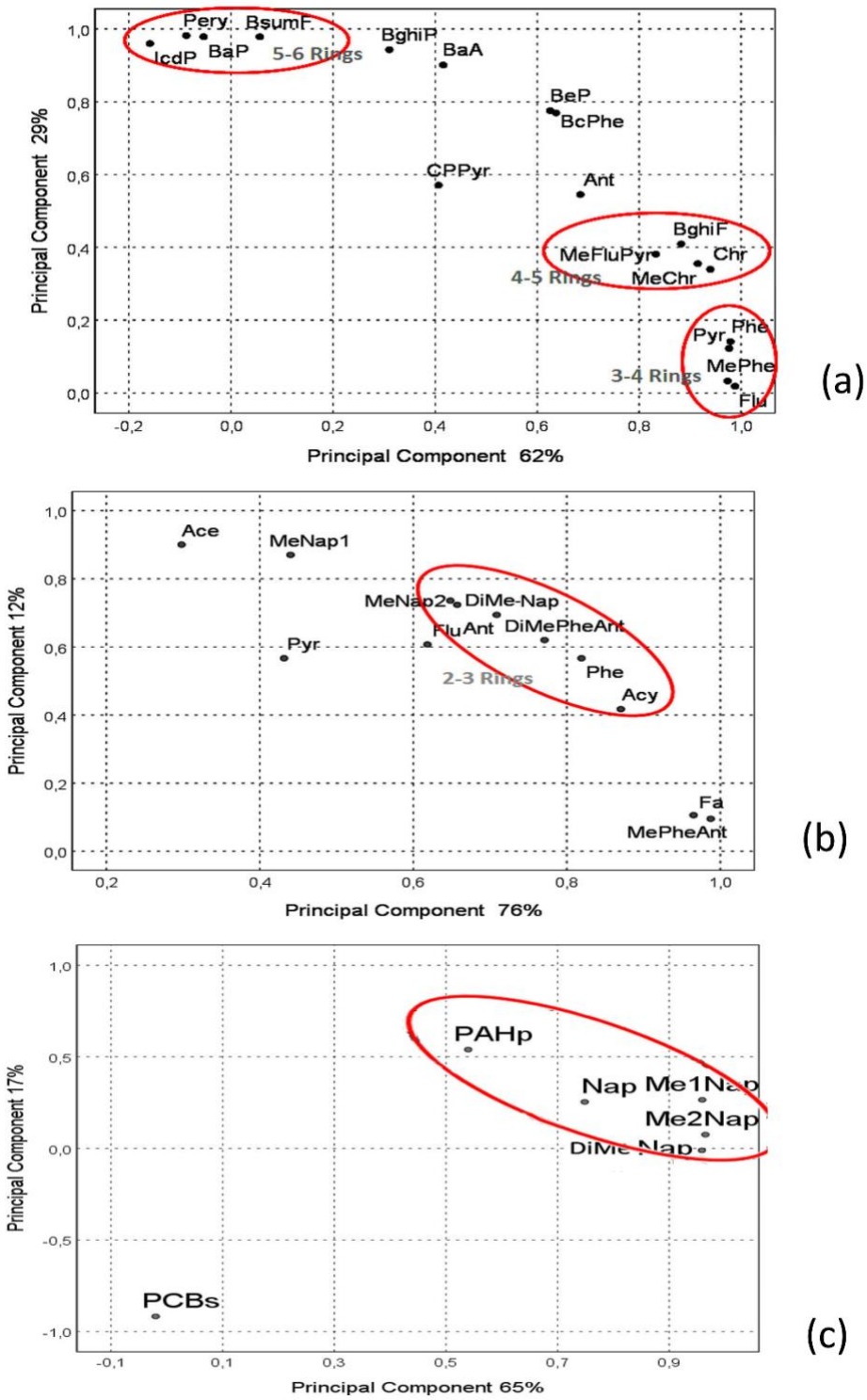

Fig. 8. Principal component analysis as loading plot of (a) 18 particulate PAHs; (b) 13 gaseous PAHs; (c) naphthalene, NAPH methylated derivatives, total particulate PAHs and PCBs, measured inside the company.

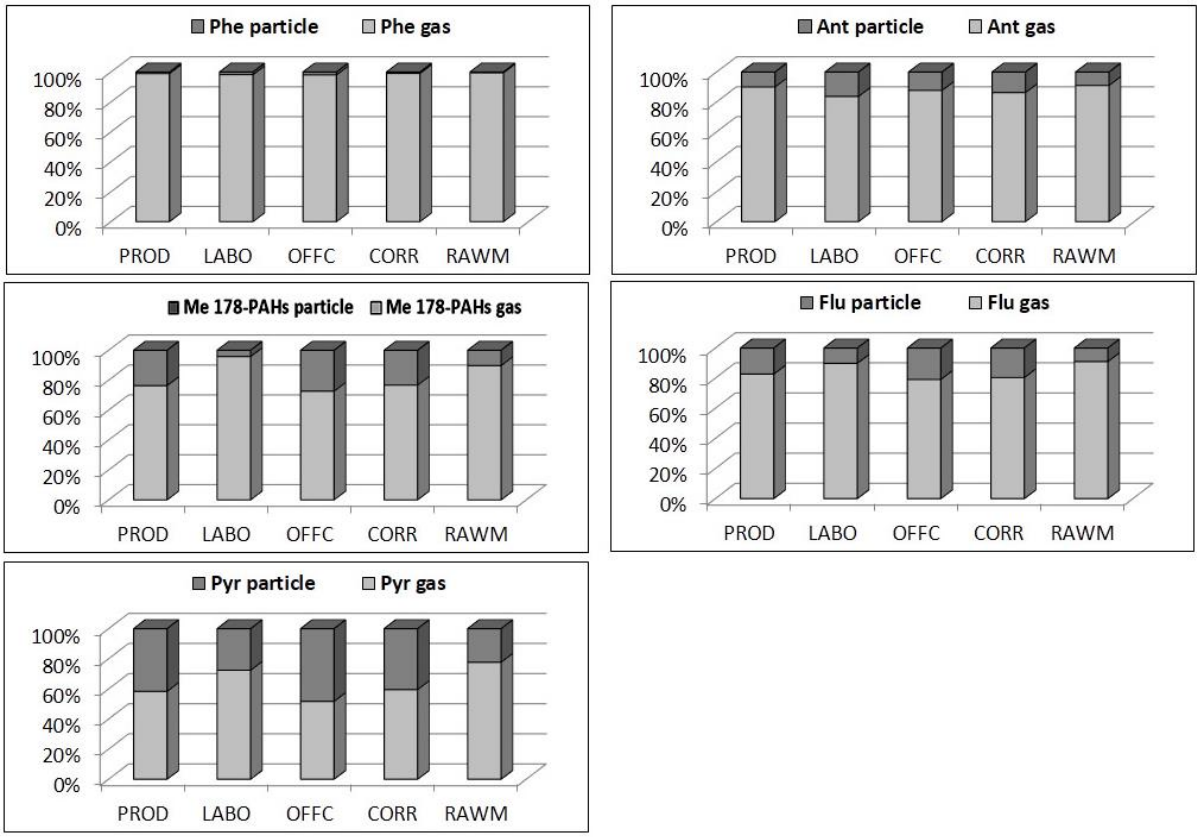

Fig. 9. Concentrations of 5 PAHs compounds in particulate and gaseous phases measured in five interiors of ENAP.

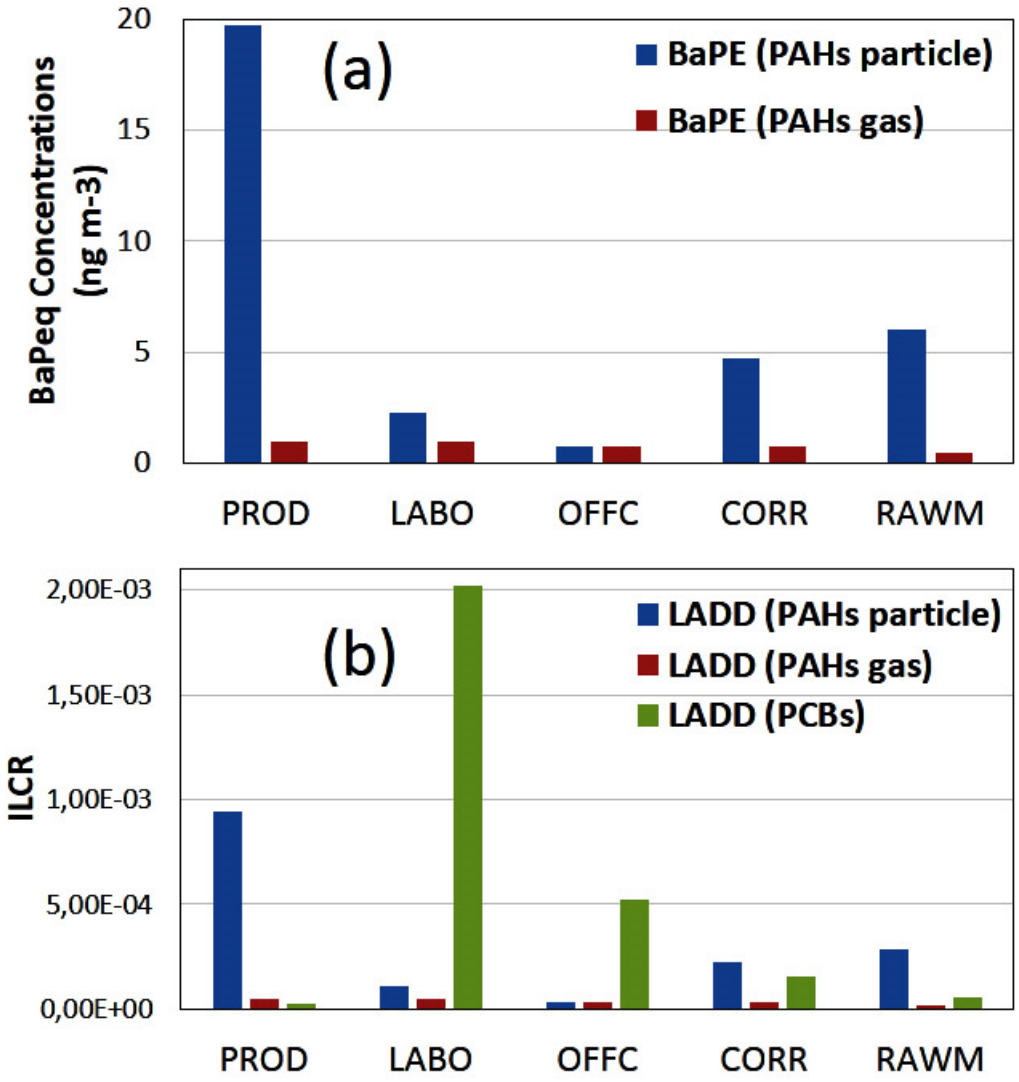

Fig. 10. BaP equivalent (BaPeq) concentrations and incremental lifetime cancer risk (ILCR) measured at the five sites inside the factory.

Supplementary Material

The assessment of organic contaminants at a paint manufacturing site: implications for health risks and source identification

By Sidali Khedidji, Catia Balducci, Lyes Rabhi, Angelo Cecinato, Riad Ladji and Noureddine Yassaa

Table SI. Description of the indoor sampling points

Sampling point	Environment	Location	Type of sampling	Description
Paint manufacturing (1)	PROD	ground floor	Active Passive	Production workshop of white emulsion products and oil-based paint
Paint manufacturing (1)	PROD	ground floor	Active	Production workshop of white emulsion products and oil-based paint
Finished product area	PROD	ground floor	Active Passive	Solvent paint production workshop all types of colored paint
Laboratory (1)	LABO	1st floor	Active Passive	Formulation development and control of raw materials with several windows in the facade of the road
Laboratory (2)	LABO	1st floor	Active Passive	Application room of the paint samples to develop with several windows in the facade of the road
Laboratory (3)	LABO	2nd floor	Active	Room application and control finished product with several windows in the facade of the road
Administrative block (1)	OFFC	1st floor	Passive	director's office, non-smoker, with 2 windows in the facade of the road, air conditioner
Administrative block (2)	OFFC	1st floor	Active	4 workers, non-smokers, with 3 windows in the facade of the road, fan coil and natural ventilation
Security	OFFC	ground floor	Active	2 workers, Smoking > 10 cigarettes per day, Natural ventilation with only window in the facade of the corridor
Corridor	CORR	ground floor	Active Passive	Corridor leads to the production workshops
Corridor	CORR	ground floor	PM_{10}	Corridor leads to the production workshops
Corridor	CORR	ground floor	Active	Corridor leads to the Raw material workshops
Solvents storage	RAWM	ground floor	Only PM_{10}	Two doors one is in the side of the corridor and other one in the resin storage workshop
Solvents regeneration	RAWM	ground floor	Active	Two doors, the presence of some trucks used to ship
Resin storage	RAWM	ground floor	Only PM_{10}	Two doors, the presence of some trucks used to ship
Powders storage	RAWM	ground floor	Passive	Two doors, the presence of some trucks used to ship

Table SII. Atmospheric concentration (ng m^{-3}) of PAH congeners in gaseous (G) and particulate (P) phases at the five sites.

PAHs	MW	PROD		LABO		OFFC		CORR		RAWM	
		G	*P*	*G*	*P*	*G*	*P*	*G*	*P*	*G*	*P*
NAP	*128*	856.9	n.e.	622.1	n.e.	899.6	n.e.	672.5	n.e.	403.8	n.e.
1-Me NAP	*142*	408.4	n.e.	297.7	n.e.	253.7	n.e.	200.9	n.e.	114.0	n.e.
2-Me NAP	*142*	204.5	n.e.	187.7	n.e.	136.5	n.e.	121.2	n.e.	69.5	n.e.
DMe NAP	*156*	735.2	n.e.	698.6	n.e.	448.7	n.e.	440.7	n.e.	214.1	n.e.
ACY	*152*	7.8	n.e.	9.2	n.e.	6.6	n.e.	7.1	n.e.	4.9	n.e.
ACE	*154*	24.4	n.e.	10.7	n.e.	8.2	n.e.	6.5	n.e.	2.1	n.e.
FA	*166*	20.1	n.e.	41.9	n.e.	10.9	n.e.	11.7	n.e.	4.9	n.e.
PHE	*178*	51.9	0.557	52.8	0.416	23.2	0.279	31.5	0.290	14.2	0.271
ANT	*178*	3.5	0.384	2.8	0.315	1.6	0.162	2.0	0.321	1.2	0.280
Me 178-PAHs	*192*	8.4	2.604	15.8	1.647	4.4	0.969	6.3	0.719	3.2	0.685
DiMe 178-PAHs	*192*	4.2	n.e.	3.9	n.e.	1.7	n.e.	2.4	n.e.	1.0	n.e.
FLU	*202*	2.3	0.475	2.0	0.319	1.2	0.222	2.2	0.215	0.91	0.230
PYR	*202*	1.4	1.005	1.1	0.646	0.69	0.379	1.6	0.446	0.56	0.426
Me 202-PAHs	216	n.e.	0.740	n.e.	0.822	n.e.	0.344	n.e.	0.393	n.e.	0.324
BghiF	226	n.e.	0.634	n.e.	0.628	n.e.	0.223	n.e.	0.339	n.e.	0.289
CPPyr	226	n.e.	0.434	n.e.	1.077	n.e.	0.200	n.e.	0.380	n.e.	0.242
BcPhe	228	n.e.	0.187	n.e.	0.183	n.e.	0.090	n.e.	0.169	n.e.	0.102
BaA	228	n.e.	0.428	n.e.	0.534	n.e.	0.188	n.e.	0.480	n.e.	0.232
Chr	228	n.e.	2.405	n.e.	1.914	n.e.	0.716	n.e.	1.132	n.e.	0.866
Me-Chr	242	n.e.	1.678	n.e.	1.509	n.e.	0.557	n.e.	0.764	n.e.	0.552
Total $\sum_{20}$PAHs		**2329**	**9.9**	**1946**	**8.5**	**1797**	**3.8**	**1507**	**4.9**	**834**	**3.9**

Symbols: G = gas phase; P = particulate phase; n.e. not examinated.